CORRELATION OF THE FRACTURE TOUGHNESS OF TITANIUM WITH MODIFIED INSTRUMENTED CHARPY IMPACT TEST RESULTS

By

John B. Einfalt

Submitted in partial fulfillment of the requirements for the Master's of Science degree.

Department of Materials Engineering

Youngstown State University

Youngstown, Ohio

May, 1988

Approved: Robert A. McCoy
Advisor

Richard W. Jones
Department Head

Sally M. Hotchkiss
Dean of Graduate Studies

TABLE OF CONTENTS

ABSTRACT

Twenty samples of Titanium 6Al-4V alloy of three different heats were tested with the purpose of finding a correlation between fracture toughness and the results of instrumented Charpy impact tests with some modifications. Using methods of absorbing vibrations of the specimens during impact had no definite effect on the final results but did improve the smoothness of the Load versus Time curves. Some correlation was found between specimens with similar microstructure and heat treatments but excessive scatter was found when a correlation was attempted with all of the heats. From SEM examination, no difference could be seen in the fracture surfaces of the two similar heats even though they had different fracture toughness values. The third heat, however, showed a great difference. It was concluded that Charpy test results of specimens of different microstructures may be difficult to correlate with fracture toughness but it is possible that the amount of plane strain fracture can be used to find a correction for an accurate correlation.

INTRODUCTION

The objective of this thesis was to investigate the relationship between plane strain fracture toughness and the results of instrumented Charpy impact tests of metals. Specifically, a Ti-6Al-4V alloy was investigated with some variations in testing and with several methods of correlation.

A total of 20 specimens were tested with 11 being precracked and the remaining being standard (non-precracked). The specimens were taken from three different heats with two heats being from plates and the third heat being from a billet. All of the specimens were taken from tested compact tension specimens and machined in the T-L direction. Refer to Table I for a summary and Figures 1, 2, and 3 for micrographs of each heat.

The three heat treatments of these samples were chosen to give each group different fracture toughness characteristics. The 870488 heat has a high fracture toughness since it was taken from a rolled plate and solution treated, annealed, and then given a heat treatment to allow the grains to become more equiaxed.[1] In other words, a highly worked material was treated to relieve some of the stresses and to allow a more ductile and tough microstructure to form. The 880423 heat is the least tough because it was taken from highly worked plate, solution treated and annealed. This left a less tough microstructure than the 870488 heat since the grains had less opportunity to form an equiaxed grain structure. The 870494 heat had a high toughness because it was taken from an extensively forged billet[1] and given a heat treatment that formed a martensitic alpha phase which was then aged to form equilibrium alpha and beta phases.[2] This caused an increase in the toughness and strength of this alloy. The microstructure of this heat showed large, equiaxed grains with

finely distributed particles of the beta phase.[2] Refer to Figure 26 for a phase diagram to explain these heat treatments further.

Equipment modifications were made with the purpose of reducing the oscillations which commonly appear on Load versus Time curves of Charpy tests. These oscillations are caused by the vibration of the tup during impact and can interfere with the accurate interpretation of these curves.[3] The modification used was to place a piece of electrical tape over the striking area of the tup which then theoretically absorbed some of the vibrations of impact. Comparison tests were made with different variations of this modification.

LITERATURE REVIEW

Plane strain fracture toughness (designated as K_{IC}) is an important material property used in the design of many mechanical components where it is important to know the conditions under which fracture will occur.[4] In simple terms, it is the value of the stress intensity at a crack tip that will cause unstable crack propagation.[4] K_{IC} is related to the stresses and the maximum flaw size present in a component and so can be used both for design and to select the most suitable material for a certain application. The common methods currently approved for the measurement of K_{IC}, such as the compact tension and the bend specimen methods, are somewhat expensive and inconvenient, so there has been interest in using other methods.[5]

One common method being considered as an alternative is the Charpy impact test which has many advantages, "such as ease of preparation, simplicity of test method, speed, low cost in test machinery, and low cost per test".[4] The Charpy test is now usually instrumented with strain gages and computerized so that graphs showing the load on the tup versus time and the total culmulative energy versus time can be immediately plotted after a test. This gives the Charpy test the advantage of being an efficient way to obtain a large amount of information about a material's fracture properties quickly.[4]

There are, however, several objections to using a Charpy test to measure fracture toughness. For one, a Charpy test uses a test specimen that is relatively small and of a simple shape as compared to an actual engineering component or even to a conventional toughness specimen.[4] This continually raises the question of how a material may behave differently depending on its size and shape. One important aspect of this is the plane stress versus plane strain condition. Since the plane strain fracture mode will give a more

conservative fracture toughness value,[4] it is necessary to insure that fracture toughness testing is done in this mode. Refer to Figure 27. Normally, for many metals without a large amount of ductility, the Charpy test specimen will fail by plane strain fracture which is inherently true because of its square cross-section (which gives a large relative thickness).[4] The degree of plain strain fracture present can be judged by the percent of flat fracture versus slant fracture of a tested specimen. With a large amount of flat fracture, plane strain conditions can be assumed to be present.[4]

The Charpy test is also different from conventional fracture toughness testing in that it is an impact test unlike conventional testing which uses quasi-static loading.[6] This can cause difficulties because the analysis of fracture behavior under high loading rates is complex and not well understood. Inertial loads and vibrations interfere with being able to accurately represent the fracture process with graphs and makes their interpretation difficult.[7] Also if a material is strain-rate sensitive, then impact loading may cause the apparent fracture toughness to be different from quasi-static loading.[8] For many metals, such as ferritic and pearlitic steels, fracture toughness has been found to decrease with increasing strain rate because the deformation of microcracks is enhanced.[8] Unfortunately, other research has found some strain rate dependence of the Ti alloy tested in this paper which has meant a higher apparent fracture toughness,[9] and this may cause difficulty when correlating impact test results to fracture toughness values.

Another reason for hesitation in using the Charpy test for fracture toughness measurement is that it was originally meant only as a method to find the brittle to ductile transition temperature of metals.[10] The results of Charpy testing are often looked upon as being values to compare the usefulness

of different materials for a certain application, and not as being able to yield a specific material property value such as fracture toughness. Again, much of the reason for this is the unpredictability and complexity of test results due to the nature of impact loading.[6]

In many cases the fracture resistance of an impact-load specimen is usually lower than that of a conventional test, and so this would mean a conservative fracture toughness value.[4] Also, for engineering components that will experience impact loads in service, the impact-load test may have greater meaning when used in design. So, despite the difficulties in interpreting results, there is great hope in finding methods to measure fracture toughness with the Charpy test.

A very important variation of Charpy testing is that specimens may be precracked to eliminate the energy needed to initiate a crack during the test.[4] Precracking gives a more accurate account of the energy needed for crack propagation but still does not eliminate inertia or vibrational effects from the test results. Also, precracking adds some difficulty to preparing specimens since a method to induce a fatigue crack is needed and so the cost of the specimen may be doubled.[11] In general the precracked Charpy test is thought to give a more accurate correlation with fracture toughness than the standard test[9] and still is very economical.

For this thesis, three methods were considered to find a correlation of fracture toughness to the Charpy test results. One of these used the relation:

$$K_{IC}^2/E = A(CVN_1)^n$$

where A and n are constants, CVN_1 is the energy of fracture, and E is the material's modulus of elasticity.[6] This correlation has been used with some success with steels[6] but apparently has not been tried with titanium alloys

which may be due to their strain rate sensitivity. The term K_{IC}^2/E is called the static fracture toughness parameter and the constants A and n are calculated by comparing CVN_1 values to previously tested K_{IC} values. Other research has found that n = 1 since K_{IC} is found to be proportional to $(CVN_1)^{1/2}$ and this will be assumed for this paper too.[9] The CVN_1 value is found from the load versus time curve as the energy of crack propagation.[6] For a Charpy test with a precracked sample this is the total energy or the total area under the curve. For a standard sample test, this is the area under the part of the load versus time curve that represents only the energy of crack propagation, not including the energy of crack initiation. See Figure 28 for a further explanation of this. Since all of the specimens compared in this paper had the same value of E, the correlation can be simplified as:

$$K_{IC} = B\ (CVN_1)^{1/2}$$

where B is found from a curve of K_{IC} versus $(CVN_1)^{1/2}$.

A second method of correlation suggested by other researchers is to calculate the plane strain dynamic fracture toughness, K_{ID}, and then to find a correlation of this parameter to K_{IC}.[9] K_{ID} is a similar material property parameter as K_{IC} except that it is defined in terms of impact test results. For materials that are not strain rate sensitive, $K_{ID} = K_{IC}$, but for materials that are, $K_{IC} = A\ K_{ID}$ where A is an empirically derived constant.[9] A quick way of judging the amount of strain rate sensitivity of an alloy is by noting how large the shear lip area is on the fracture surfaces of a Charpy specimen.[9] A greater shear lip area means a greater strain rate sensitivity and K_{ID} will be greater than K_{IC}.[9] To calculate K_{ID}, this equation was used:

$$K_{ID} = [(E/(1-v^2))\cdot(W/A)]^{1/2}$$

where v is Poisson's ratio, E is the modulus of elasticity, and W/A is the

energy to maximum load per unit area for the propagation energy.[9] Since in all cases the cross-sectional area of the specimens was 1 cm^2 = 0.155 in^2, then W/A= W/0.155. For precracked Charpy tests, W was found as the area under the load versus time curve up to maximum load. For standard Charpy tests, W was estimated as being 1/2 of the value of CVN_1 found as described previously.[9] Since all of the samples compared in this paper have the same values of E and v, this correlation can be simplified as:

$$K_{IC} = B\ K_{ID} = B\ [W/A]^{1/2}$$

A third method of correlation is known as the Rolfe-Novak-Barson correlation and is stated as:[5]

$$[K_{IC}/YPS]^2 = 5/YPS\ [CVN_2 - (YPS/20)]$$

Here, YPS is the yield point strength and was different for each heat as shown in Table I. CVN_2 is the Charpy energy but is different from CVN_1 because it is calculated as the cumulative energy after the maximum load and can be found for only standard tests.[5] See Figure 29. This relation is empirically derived and based upon many tests of different materials. It has been found to have good agreement with low alloy, high alloy, and carbon steels but no mention was made regarding titanium alloys.[5] The parameter YPS is used so that a relationship can be found between materials of different strengths. This correlation can be judged to be accurate if a graph of $[K_{IC}/YPS]^2$ versus CVN_2/YPS yields a straight line, such as shown in Figure 30. For comparison, this correlation can be simplified as:

$$K_{IC} = [5 \cdot YPS \cdot CVN_2 - (YPS)^2/4]^{1/2}$$

As shown in Figures 28 and 29, one advancement made by instrumenting the Charpy test has been the ability to calculate more accurately the values of CVN and W. This is not only because the load versus time curve of the Charpy

test shows the actual crack propagation energy, but also because the extraneous loads that occur can be identified. Once the extraneous loads are identified, their energy contributions can be subtracted from the total energy to get a true energy to maximum load value. For non-strain rate sensitive materials, if the true energy for fracture can be found, then this should be equal to the energy for fracture for quasi-static loading which is used to calculate K_{IC}.

The most prominent extraneous load usually found is that from inertia, or the force used to accelerate the specimen when impacted by the tup.[4] This extraneous load is normally present on the load versus time curve as a small peak at the beginning of the curve[9] and its energy contribution is easy to evaluate. For standard Charpy tests this extraneous load does not contribute to the value of CVN or W and can be neglected.

There are many other types of extraneous loads, most of which result from vibrations of the tup during impact and they are present along the entire load versus time curve. Normally the amplitude of these vibrations can be minimized by reducing the speed of impact[3] but this can add uncertainty when comparing results to other tests and difficulty in performing the impact test. Part of the research for this paper involved evaluating different methods of absorbing the vibrations of the tup so that a more accurate load versus time curve could be obtained and therefore more accurate CVN and W values could be calculated.

PROCEDURE

All of the equipment used for this research was located at the Youngstown State University. The impact testing unit used was a Dynatup model ETI-630 which consisted of a central data processor, disk drive system, CRT, printer, and a Tinius Olsen 300 ft·lb capacity impact testing machine. The testing machine was conventional except that the tup (the part of the hammer that strikes the specimen) had two strain gages mounted in grooves on its side to measure force during impact. Also, the testing machine had an electronic flag mounted on the base so that the speed of the hammer could be measured during impact. The speed of the hammer at impact was normally between 18.28 and 18.37 ft/sec and the energy of the hammer at impact was between 310 and 315 ft·lb.

Before the titanium specimens were tested, different materials were tried on the tup and tested with steel specimens to evaluate their effectiveness at vibration reduction. Materials considered included electrical tape, foam weatherstripping, packing tape, and masking tape. After many tests on steel samples, the electrical tape was found to be the most satisfactory in helping to produce a smooth load versus time curve. Electrical tape was also tested wrapped around the Charpy specimen at both ends with the intent of absorbing vibrations between the specimen and the anvil of the base of the testing machine. This was found to have no effect on the results so it was never tried with the titanium samples.

An interesting effect was found when tape was used on the tup. When a specimen was broken for the first time by a tup with tape, no improvement in the smoothness of the load versus time curve was seen in any cases. But, from

the impact, the tape was torn in the middle and folded back to form a fold of tape on each side of the tup. If another test was run with the tape left on the tup in this condition, a smoother curve would result. This was most likely because the folds of tape on the tup contacted the specimen first and acted to absorb some vibration during impact. The tape had this effect for only two or three tests and then had to be replaced. Figures 24 and 25 show progressive testing with the same pieces of tape on the tup. For all of the titanium samples tested with tape, a test was run first using a steel sample to set the tape in this desired condition.

All of the fracture surface micrographs were taken with a Hitachi scanning electron microscope and all of the photomicrographs of the grain microstructure were taken with a Zeiss metallogragh. Etching for the photomicrographs was done chemically with 10% HF-5% HNO_3-85% water.

Percent flat fracture as listed in Table II was measured using a venier caliper to measure the width of the slant fracture zone on each side of each specimen. Since the width of the specimen was 1 cm, subtracting this value from 1 and multiplying by 100 gave the percent flat fracture.

DISCUSSION OF RESULTS

The results from all of the Charpy tests are shown as load and energy versus time curves in Figures 4 through 23. In each case the load referred to is the instantaneous force measured on the tup of the hammer by the strain gages. The energy referred to is cumulative and so at a given instant represents the total area under the force versus time curve up to that point. The curves are identified by heat of material, as being standard or precracked, and as to whether tape was used on the tup or not.

Table II gives a summary of the test results. As shown by the values for the percent flat fracture, the 870494 heat had almost all plane strain fracture while the 870488 and 880423 heats showed some deviation from the plane strain fracture mode. This can be explained by the fact that the 870494 heat had a microstructure of large, equiaxed grains which promoted flat fracture. The other two heats showed some shear lips partly because they each still had a mostly deformed, elongated grain microstructure and also due to the orientation of the fracture to the grains. In all cases, precracked samples had a greater percent of flat fracture than standard samples demonstrating an important advantage of precracking in promoting the plane strain fracture mode.

By comparing the results in Table II and the curves in Figures 4 through 23, the effectiveness of using tape on the tup can be determined. In nearly all cases a definite smoothing effect was seen by using the tape. An exception to this was specimen 18 (Figure 21) which may have been caused by improper mounting of the tape. A definite trend was that the tape smoothed the first part of the curves up to the maximum load, but did little to change the oscillating nature of the rest of the curves. So, the use of tape has its

greatest effect in dampening the inertia load and other vibrations occurring before the maximum load. For standard samples this is of little value since CVN and W/A are calculated from the portion of the curve after crack initiation. For precracked samples, however, this may be important since the entire curve is used to calculate CVN. But when comparing the CVN values of tape versus no tape for both standard and precracked samples, no real difference was seen for tape versus no tape. In conclusion, using tape on the tup apparently had no effect on the final values obtained from these Charpy tests. Of course the sample size of this research was small, so further work might reveal a more positive conclusion.

Figure 31 shows curves of K_{IC} versus $[CVN_1]^{1/2}$ for both standard and precracked samples which were plotted by the first correlation method described where $K_{IC} = B\ [CVN_1]^{1/2}$. The points plotted do not show a linear relationship as had been hoped except if the averages of the points for each heat are taken as shown by the line in Figure 31. The failure of this plot can be explained partially by the fact that the 880423 and 870488 heats showed a fairly large amount of slant fracture which means they probably did not fail in the plane strain fracture mode. Therefore, they probably possessed a greater K_{IC} value than their true value as explained by Figure 27.[4] This appears to be true for the points plotted for the standard specimens but unfortunately the opposite is shown for the precracked specimens.

In the case of the standard specimens, the deviation from plane strain fracture can be accounted for by decreasing the values of $(CVN_1)^{1/2}$ for the 880423 and 870488 heats so that a linear relation is obtained. Of course, since there are only three points, this is an arbitrary solution but it suggests that percent flat fracture could be included as a variable in any

correlation where the plane strain fracture mode is not always present. For the data points in Figure 31, if the $[CVN_1]^{1/2}$ values for the 870488 and 880423 heats were each decreased by 0.4 $(ft \cdot lb)^{1/2}$, then a linear relation resulted as shown in Figure 32. Values for both heats were decreased the same amount because both showed the same percent flat fracture and would be expected to have the same increase in plane strain fracture toughness. This is a 16% decrease which may be related to the 25% of slant fracture that each group of specimens had shown. Therefore, a proportional relationship might be found between percent slant fracture and the increase in apparent plane strain fracture over its real value. For the curve shown in Figure 32 a value was added to $B[CVN_1]^{1/2}$ since the K_{IC} axis intercept is not equal to zero. Taking this into account, the final correlation is:

$$K_{IC} = 90(CVN_1)^{1/2} - 109$$

For the precracked data points shown in Figure 31, there is no apparent explanation as to why the 870494 heat had a much greater calculated fracture toughness value and this sheds some doubt on the explanation for the deviation of the standard specimens. Using heats with a wider range of fracture toughness values may show some important trend such as a fundamental difference between the fracture mechanics of precracked and standard specimens. Another probable explanation is that it may be an unsound practice to try to compare specimens with very different heat treatments since the microstructure varies greatly and will fracture in a different manner.

It is encouraging to note that the standard and precracked points for the 880423 and 870488 heats agree very well. This may mean that standard samples can be used with accuracy with this type of correlation for fracture toughness.

Figure 33 shows curves of K_{IC} versus calculated K_{ID} values for standard and precracked samples plotted according to the second correlation method described with K_{IC} versus K_{ID}. Of course, the same scatter in the data points was present as in the first correlation since this correlation depends upon $(W/A)^{1/2}$ which is related to $(CVN)^{1/2}$. Because of this relation, the same explanations used for Figures 31 and 32 pertain to Figures 33 and 34. In other words, if the K_{ID} values of the standard specimens for the 880423 and 870488 heats each are decreased by 3.1 ksi$[in]^{1/2}$ as shown in Figure 34, then a linear relation results. Again, a factor must be subtracted to express this linear relation and the resulting correlation is:

$$K_{IC} = 12.4\ K_{ID} - 118$$

Because the values of K_{ID} were much less than the true K_{IC} values, all three of these heats have shown a large amount of strain rate sensitivity. But this does not explain the 870494 heat which should have shown no strain rate sensitivity due to its high percent flat fracture. So, for this alloy, judging strain rate sensitivity by percent flat fracture may not be valid. Also, there is much greater scatter between the standard and precracked points as compared to Figure 31 which questions the validity of the method used to find W.

The third method of correlation can be summarized by using a graph of $[K_{IC}/YPS]^2$ versus CVN_2/YPS to relate different materials as shown in Figure 30. The values for the 880423 and 870488 heats are fairly close to this curve but the 870494 heat shows a much lower relative CVN_2 value than when compared to the curve. Again, since the 880423 and 870488 heats showed some slant fracture, their CVN values may be less so their points would be plotted farther above the curve. If this thinking is correct, it suggests that this titanium alloy has a greater K_{IC}/YPS ratio or greater relative fracture resistance when

compared to alloy steels of the same yield strength.

The SEM photomicrographs of fracture surfaces of a sample from each heat are shown in Figures 35, 36, and 37. Figure 35 shows a sample from the 870488 heat at magnifications of 140X and 1400X. Both of these show almost all ductile fracture by their dimpled appearance but there is less dimpling in the precracked zone versus the fast fracture zone which is expected. Figure 36 shows a sample from the 880423 heat at the same magnifications. The same features as shown in Figure 35 are shown in these micrographs with no real differences apparent despite the difference in fracture toughness. But, this is expected too since these heats had the same percent elongation and should then show the same relative ductility.

Figure 37 shows a sample from the 870494 heat in magnifications of 40X, 140X, 720X, and 1400X. At the lower magnifications, large flat areas are seen which indicates failure by cleavage or brittle fracture. This agrees with the previous observation that the percent of flat fracture was nearly 100. At the high magnifications dimpled surfaces can be seen which may explain why this material has a high fracture toughness despite the appearance of brittle fracture at low magnifications.

CONCLUSION

Using tape on the tup was found to produce a smoother load versus time curve for Charpy tests of titanium samples. However, since no difference in the accuracy of the resulting CVN or W values could be seen, using tape had no apparent benefit.

The percent flat fracture for the 880423 and 870488 heats was lower than that for the 870494 heat which suggested that they did not fracture in the plane strain mode. Therefore, it was assumed that their K_{IC} values were less than what was indicated by the test results. This seemed to be confirmed when looking at the results of the standard tests but was contradicted by the results of the precracked tests. Still, it may be possible to calculate the effect of percent flat fracture on the change in fracture toughness over its real value if more samples are tested.

The large amount of scatter of the standard and precracked test results for the 870494 heat indicates that the Charpy test is sensitive to precracking for this alloy with a microstructure from a beta heat treatment. The other two heats with a much finer microstructure showed little difference between standard and precracked results.

In all cases, the precracked specimens showed a greater amount of percent of flat fracture. This effect was because the reduced length of the fast fractured portion of the precracked samples meant a greater relative thickness. Since the CVN values were the same for both the precracked and standard samples, this offers no benefit. So, testing with standard specimens may be just as accurate and less expensive.

ACKNOWLEDGMENTS

Appreciation is expressed to the following persons:

Dr. McCoy, Advisor for this research,

Dr. Jones, for the use of the Metallography Labs,

David McNeish, for providing the titanium samples from RMI.

REFERENCES

1. McNeish, D. J., Metallurgist at Reactive Metals Inc., Niles, Ohio, personal communication, April, 1988.

2. Reactive Metals Inc., "Facts About the Metallography of Titanium", 1981.

3. Ireland, D. R., "Procedures and Problems Associated with Reliable Control of the Instrumented Impact Test", ASTM STP 563, 1974, pp. 3-29.

4. Hertzburg, R. W., "Deformation and Fracture Mechanics of Engineering Materials", Wiley, 1983.

5. Swift, R. A., "Research Tests", presented at the 1975 ASME Petroleum Division Conference, Tulsa, Oklahoma, 1975.

6. Shockey, D. A., "Dynamic Fracture Testing", Metals Handbook, Vol. 8, Mechanical Testing, ASM, 1985.

7. Saxton, H. J., Ireland, D. R., and Server, W. L., "Analysis and Control of Inertial Effects During Instrumented Impact Testing", ASTM STP 563, 1974, pp. 50-73.

8. Metals Handbook, Vol. 10, "Failure Analysis and Prevention", ASM, 1975

9. Ewing, A. and Raymond, L., "Instrumented Impact Testing of Titanium Alloys", ASTM STP 563, 1974, pp. 180-202.

10. Radon, J. C., and Turner, C. E., "Fracture Toughness Measurement by Instrumented Impact Test", Engineering Fracture Mechanics, Vol. 1, Pergamon Press, 1969, pp. 411-428.

11. Rossi, Jim, Research Engineer of Westmoreland Testing Lab, Youngstown, Pennsylvania, personal communication, January, 1987.

12. Hoover, W. R., "Effect of Test System Response Time on Instrumented Charpy Impact Data", ASTM STP 563, 1974, pp. 203-214.

13. Reactive Metals Inc., "RMI 6Al-4V", 1967.

TABLE I: SPECIMEN PARAMETERS
Material = Ti-6Al-4V

Modulus of Elasticity, E = 16,400 ksi Poisson's Ratio, v = 0.325

HEAT NO.	870488	880423	870494
PRODUCT	Plate	Plate	Billet
HEAT TREATMENT	1750F-4 HR-A.C. +1400F-1 HR-A.C. +1725F-4 HR-F.C. @100F/HR to 900F -A.C. (Soln. Treat + Mill Anneal + Grain Refinement)	1755F-4 HR-A.C. +1400F-1 HR-A.C. (Solution Treat + Mill Anneal)	1950F-1 HR-W.Q. +1350F-2 HR-A.C. (Beta Heat Treat + Age
ULT. TENSILE	137.3 ksi	138.8 ksi	142.0 ksi
YIELD	130.7 ksi	126.6 ksi	132.2 ksi
% ELONGATION	13	13	8
% RED. AREA	29	33	17
K_{IC}, ksi·in$^{1/2}$	80.9	71.0	80.0

Table II: Summary of Test Results
(All K_{IC} and K_{ID} values are in ksi·[in]$^{1/2}$)

Specimen Group	No.	PC or ST	Percent Flat Frac.	CVN_1 ft-lb	W ft-lb	K_{ID}	CVN_2 ft·lb
880423 heat K_{IC} = 71.0 YPS = 126.6 ksi $[K_{IC}/YPS]^2$=.314 CVN_2/YPS = .07	1	ST	72	5.06	2.53		7.35
	2	ST*	78	5.01	2.50		6.95
	3	ST	70	7.43	3.71		9.35
	4	ST	75	5.43	2.71		9.79
	AVG	----	74	5.73	2.86	18.4	8.36
	5	PC	80	6.49	2.52		
	6	PC*	85	6.13	1.90		
	7	PC	84	5.82	2.75		
	8	PC*	80	5.74	1.97		
	AVG	----	82	6.04	2.28	16.4	
870488 heat K_{IC} = 80.9 YPS = 130.7 ksi $[K_{IC}/YPS]^2$=.383 CVN_2/YPS = .07	9	ST	70	7.12	3.56		8.41
	10	ST*	75	5.75	2.87		9.48
	11	ST	78	5.34	2.67		8.20
	12	ST	76	6.77	3.39		10.72
	AVG	----	75	6.24	3.12	19.2	9.20
	13	PC	84	5.79	2.43		
	14	PC*	81	6.60	2.64		
	15	PC	80	6.13	2.60		
	16	PC*	84	5.92	1.82		
	AVG	----	82	6.11	2.37	16.7	
870494 heat K_{IC} = 80.0 YPS = 132.2 ksi $[K_{IC}/YPS]^2$=.366 CVN_2/YPS = .03	17	ST	98	4.00	2.00		1.79
	18	ST*	96	4.74	2.37		6.20
	AVG	----	97	4.41	4.37	16.0	3.99
	19	PC*	98	8.89	4.20		
	20	PC	100	8.20	3.39		
	AVG	----	99	8.54	3.79	21.2	

*Tape was used on the tup for these samples.

$K_{ID} = [(E / (1-v^2)) \cdot (W / A)]^{1/2} = [\ 118.30 \cdot W\ ]^{1/2}$

E = 16,400 ksi

v = 0.325

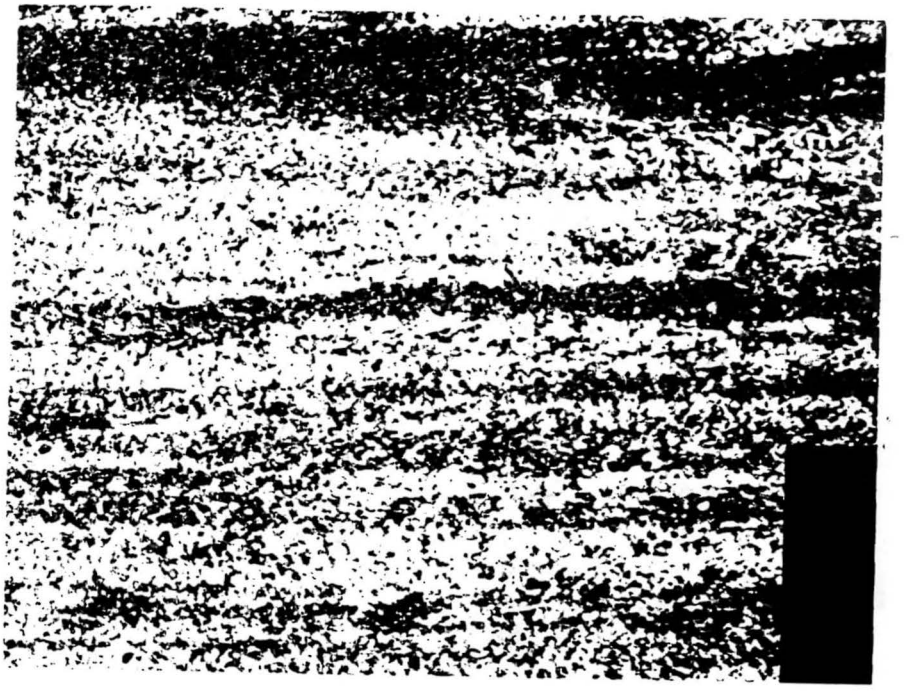

50 X

1000 X

Figure 1: Photomicrographs of heat 880423

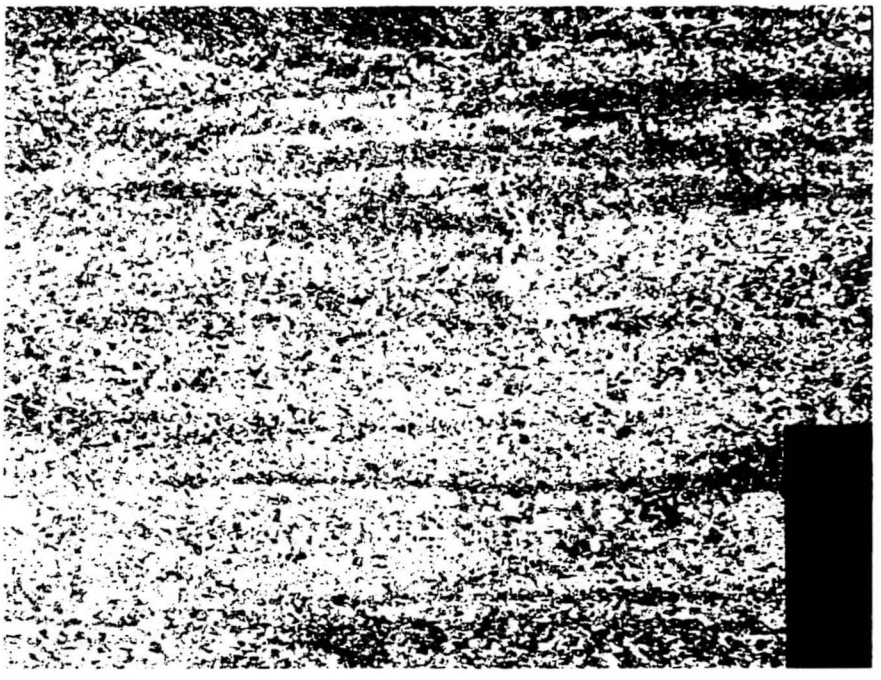

50 X

1000 X

Figure 2: Photomicrographs of heat 870488.

50 X

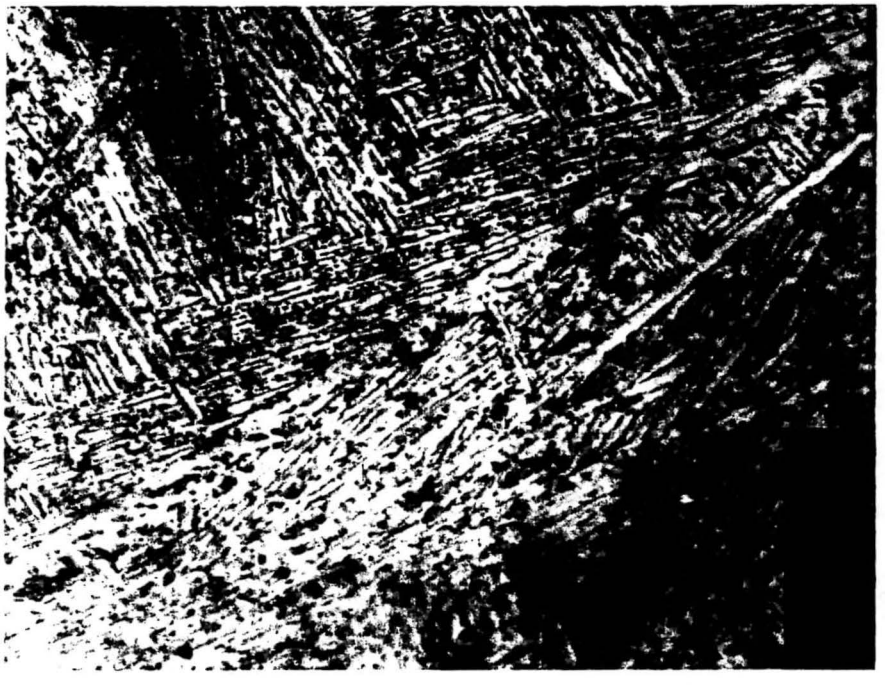

1000 X

Figure 3: Photomicrographs of heat 870494.

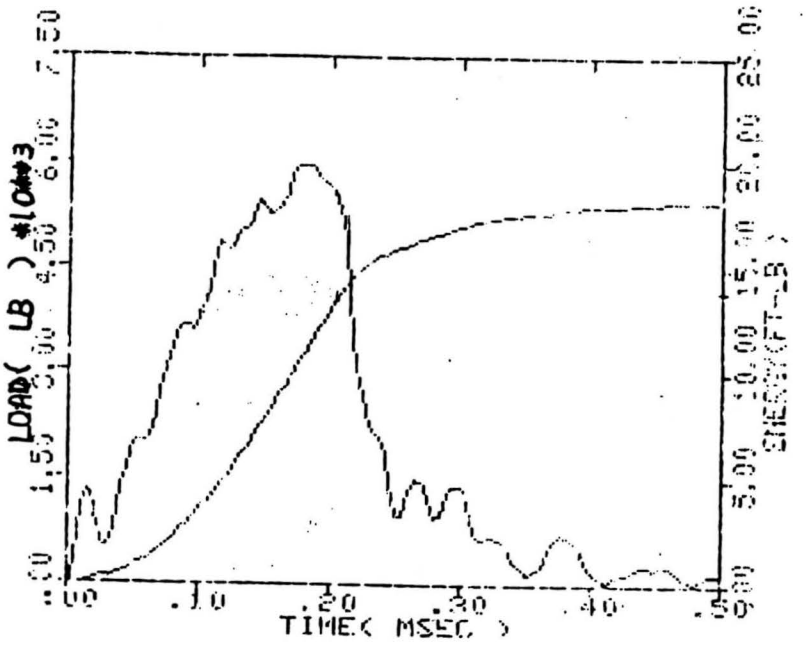

Figure 4: Specimen 1, heat 880423, standard, no tape on tup, IE=13.5 ft-lb, TE=18.56 ft-lb, CVN=IE-TE=5.06 ft-lb

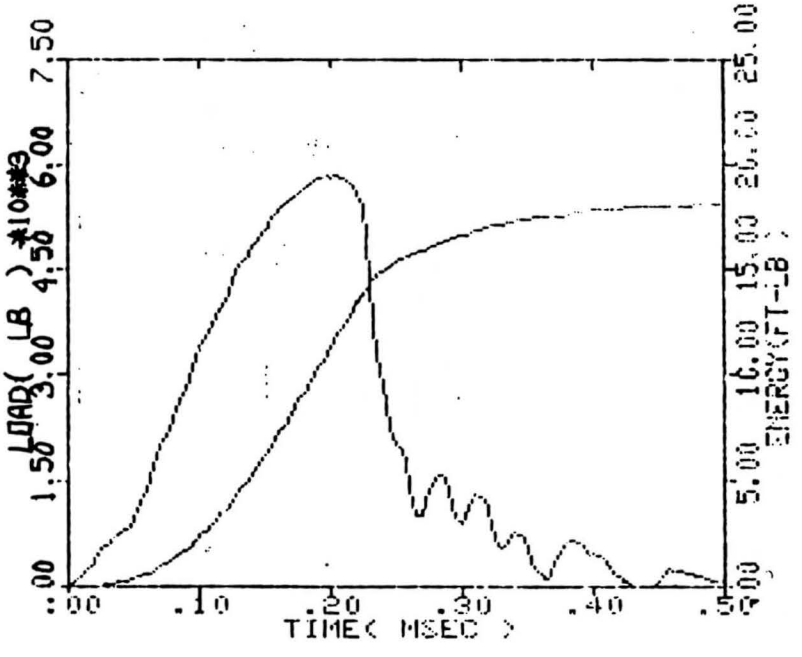

Figure 5: Specimen 2, heat 880423, standard, tape on tup, IE=13.0 ft-lb, TE=18.01 ft-lb, CVN=IE-TE=5.01 ft-lb

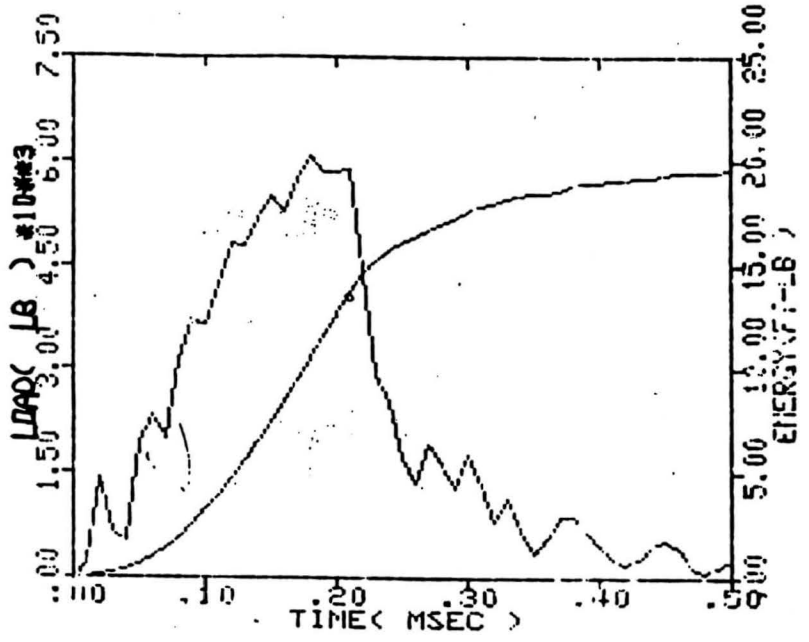

Figure 6: Specimen 3, heat 880423, standard, no tape on tup, IE=13.5 ft-lb, TE=19.93 ft-lb, CVN=6.43 ft-lb

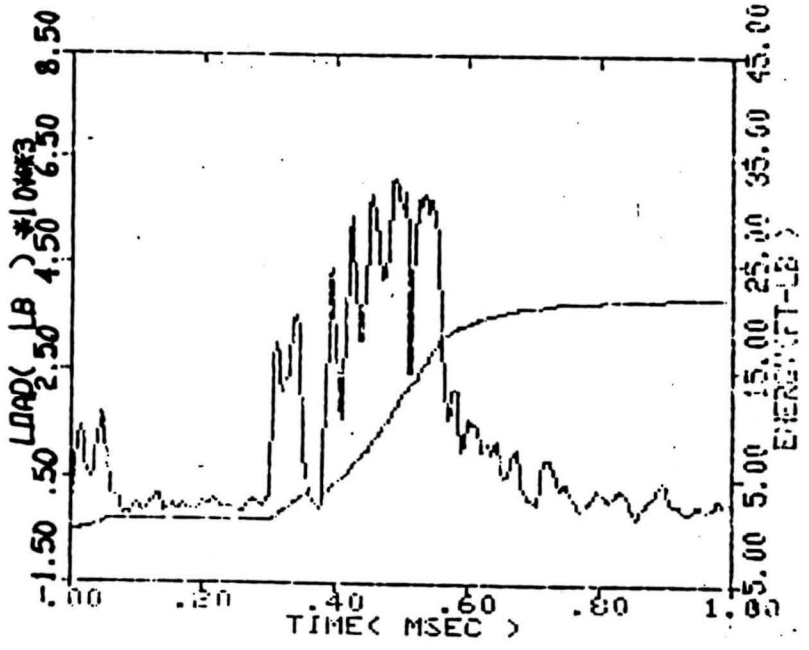

Figure 7: Specimen 4, heat 880423, standard, no tape on tup, IE=16.0 ft-lb, TE=21.43 ft-lb, CVN=7.43 ft-lb

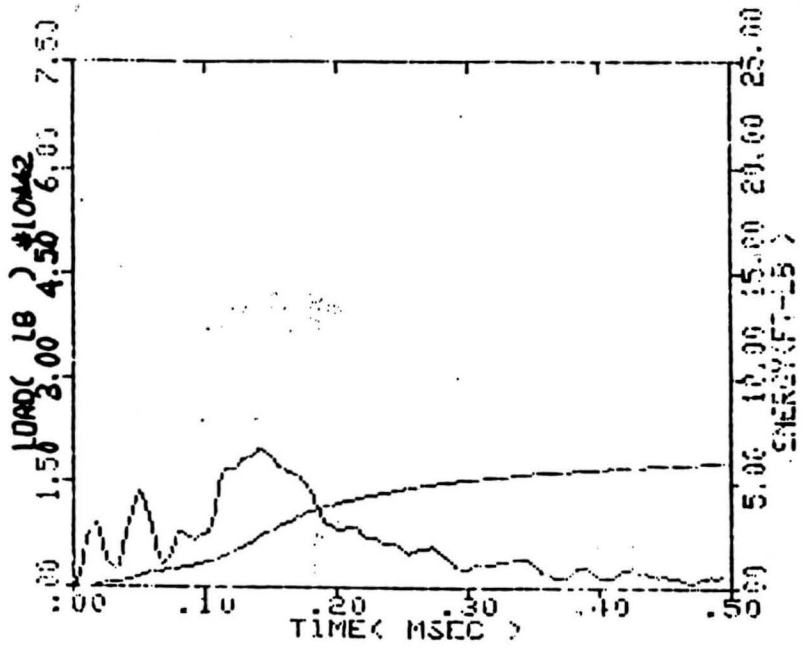

Figure 8: Specimen 5, heat 880423, precracked, no tape on tup, CVN=6.49 ft-lb

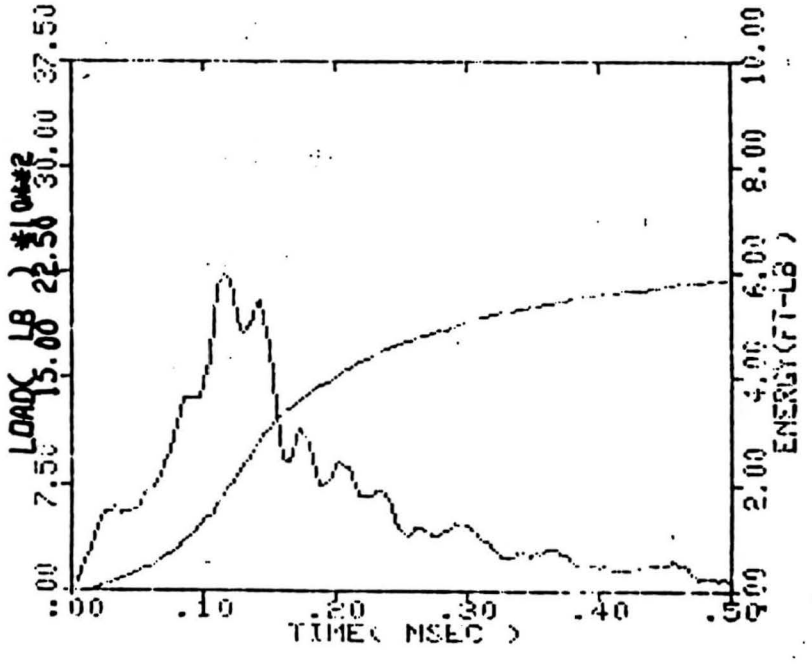

Figure 9: Specimen 6, heat 880423, precracked, tape on tup, CVN=6.13 ft-lb

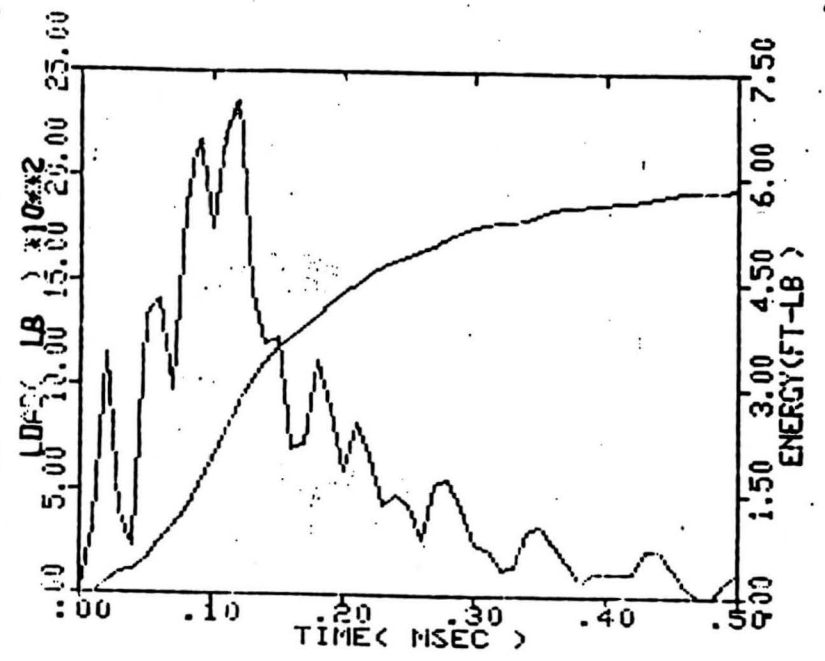

Figure 10: Specimen 7, heat 880423, precracked, no tape on tup, CVN=5.82 ft-lb

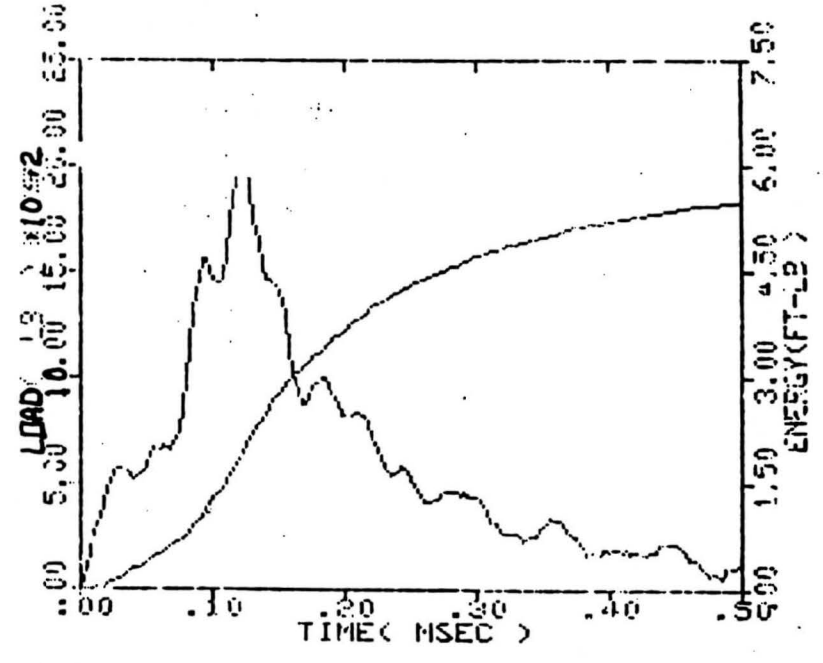

Figure 11: Specimen 8, heat 880423, precracked, tape on tup, CVN=5.74 ft-lb

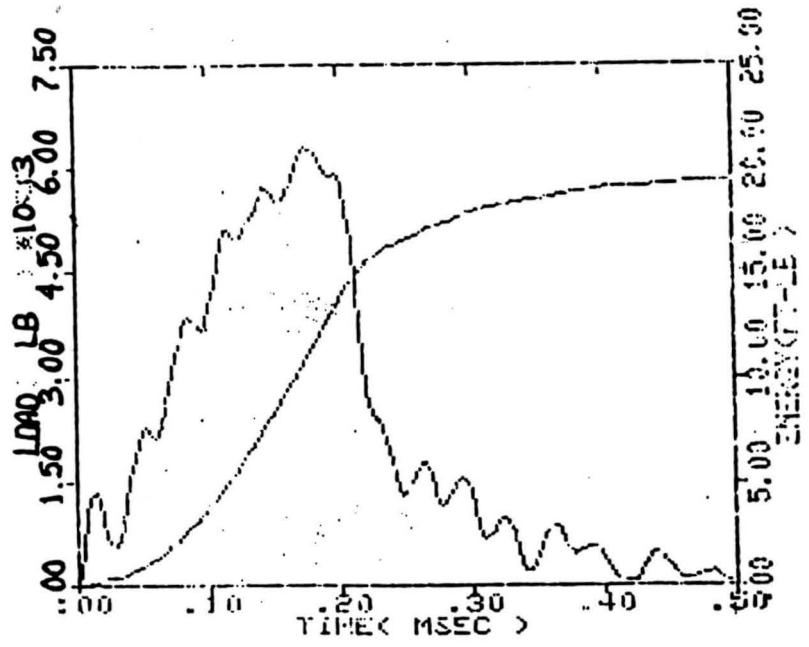

Figure 12: Specimen 9, heat 870488, standard, no tape on tup, IE=13.5 ft-lb, TE=19.62 ft-lb, CVN=6.12 ft-lb

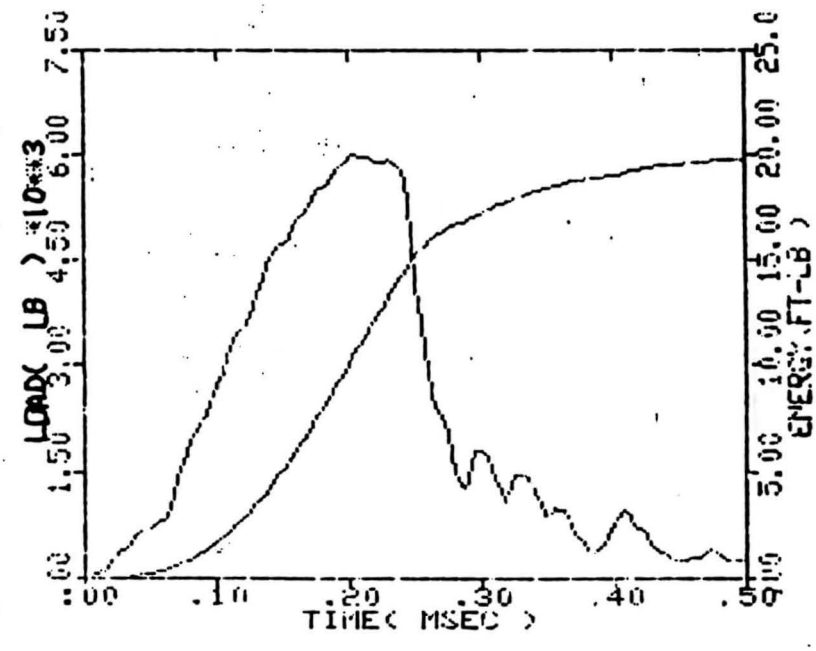

Figure 13: Specimen 10, heat 870488, standard, tape on tup, IE=14.5 ft-lb, TE=20.25 ft-lb, CVN=5.75 ft-lb

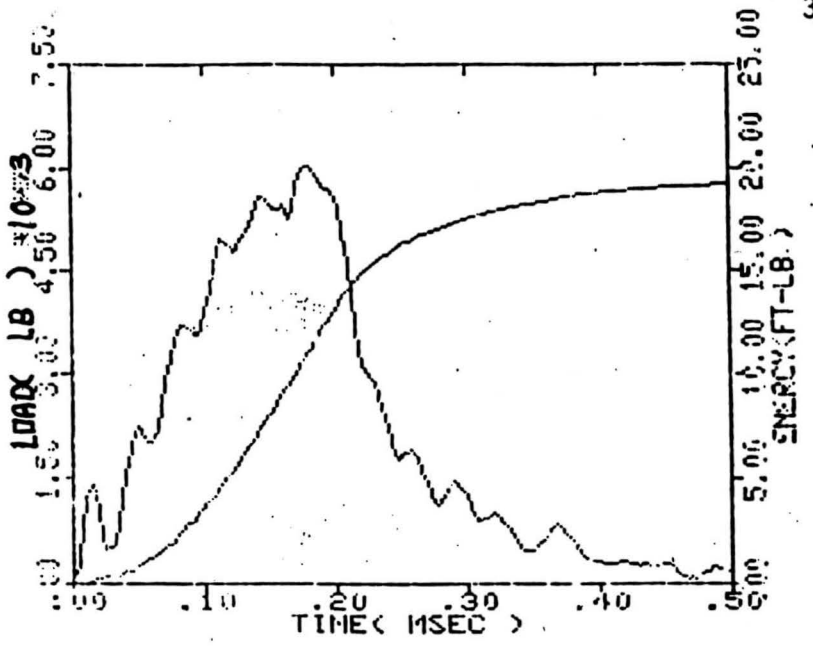

Figure 14: Specimen 11, heat 870488, standard, no tape on tup, IE=14.0 ft-lb, TE=19.54 ft-lb, CVN=5.54 ft-lb

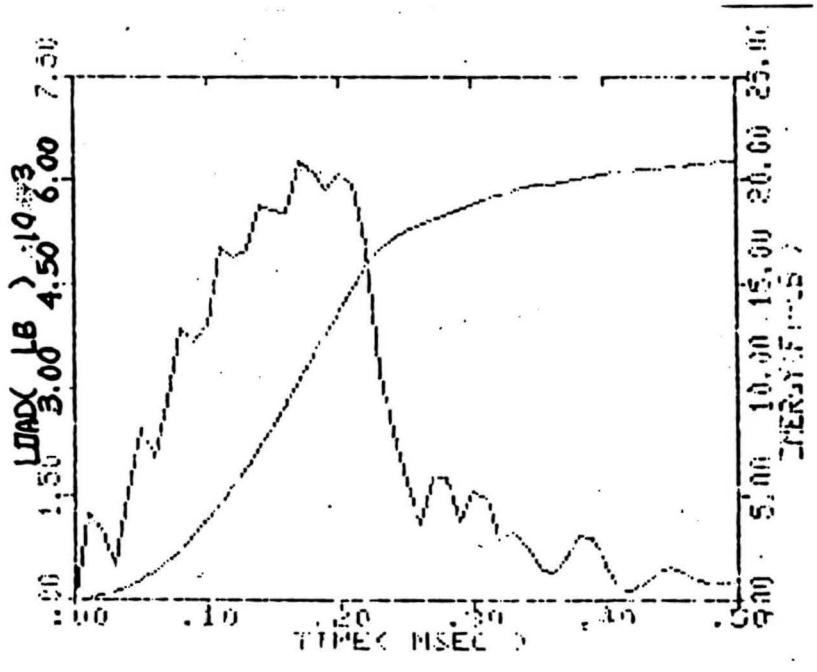

Figure 15: Specimen 12, heat 870488, standard, no tape on tup, IE=14.5 ft-lb, TE=21.27 ft-lb, CVN=6.77 ft-lb

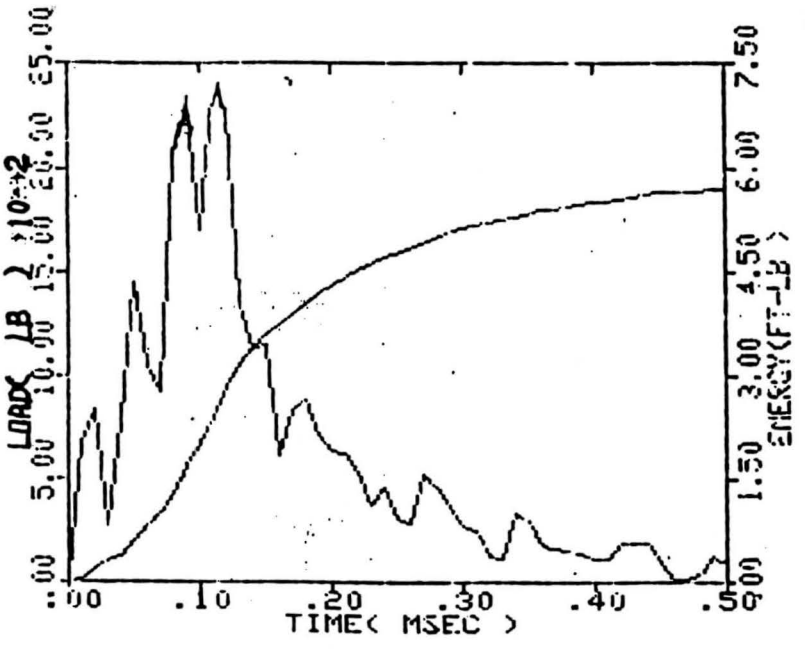

Figure 16: Specimen 13, heat 870488, precracked, no tape on tup, CVN=5.79 ft-lb

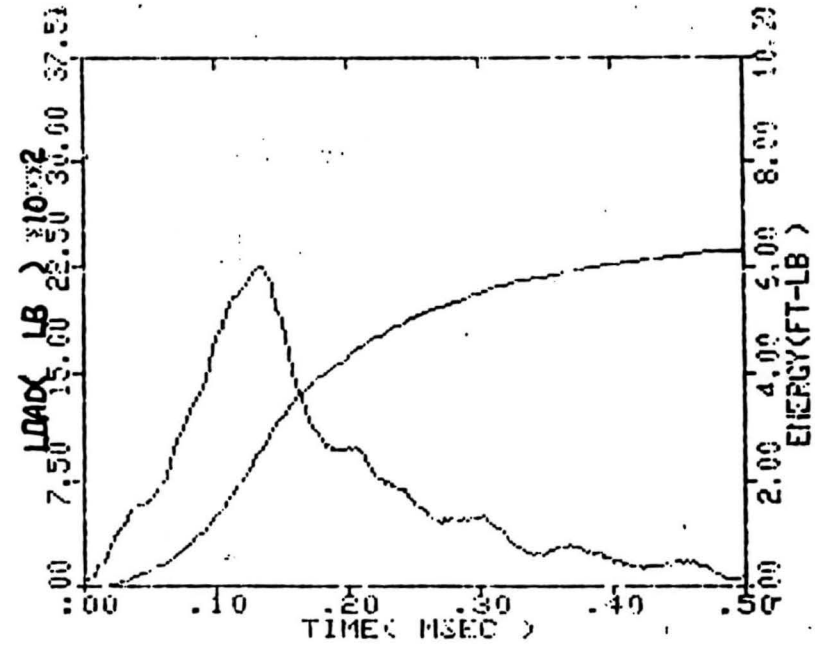

Figure 17: Specimen 14, heat 870488, precracked, tape on tup, CVN=6.60 ft-lb

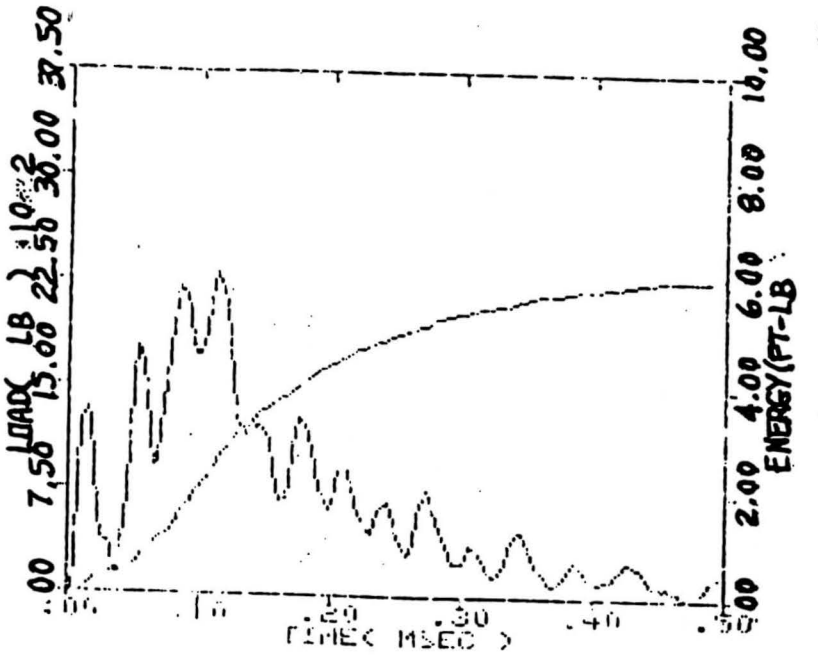

Figure 18: Specimen 15, heat 870488, precracked, no tape on tup, CVN=6.13 ft-lb

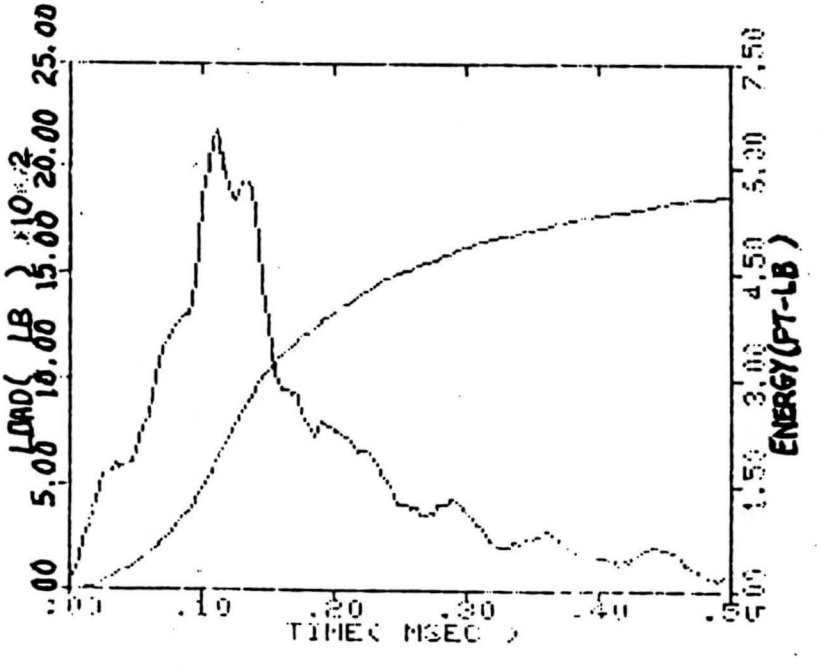

Figure 19: Specimen 16, heat 870488, precracked, tape on tup, CVN=5.92 ft-lb

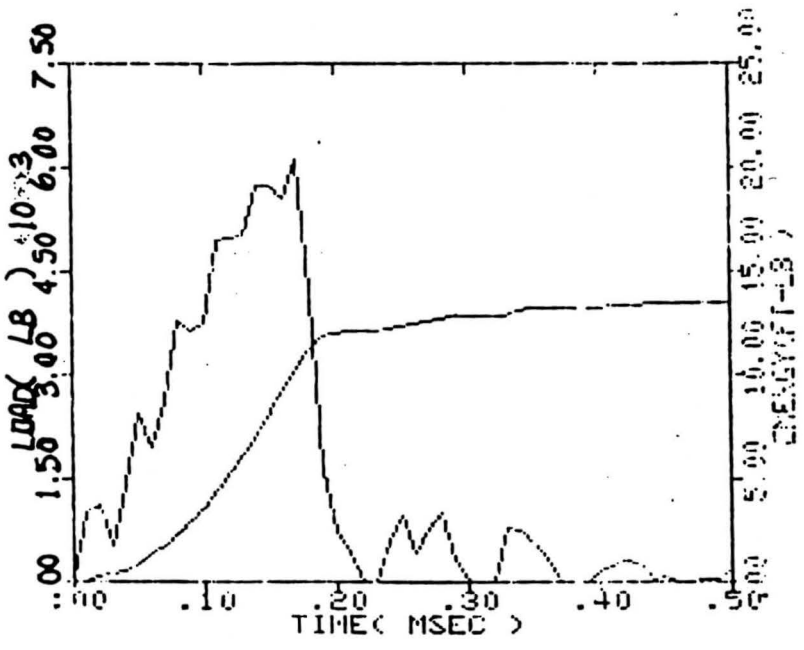

Figure 20: Specimen 17, heat 870494, standard, no tape on tup, IE=10.0 ft-lb, TE=14.0 ft-lb, CVN=4.00 ft-lb

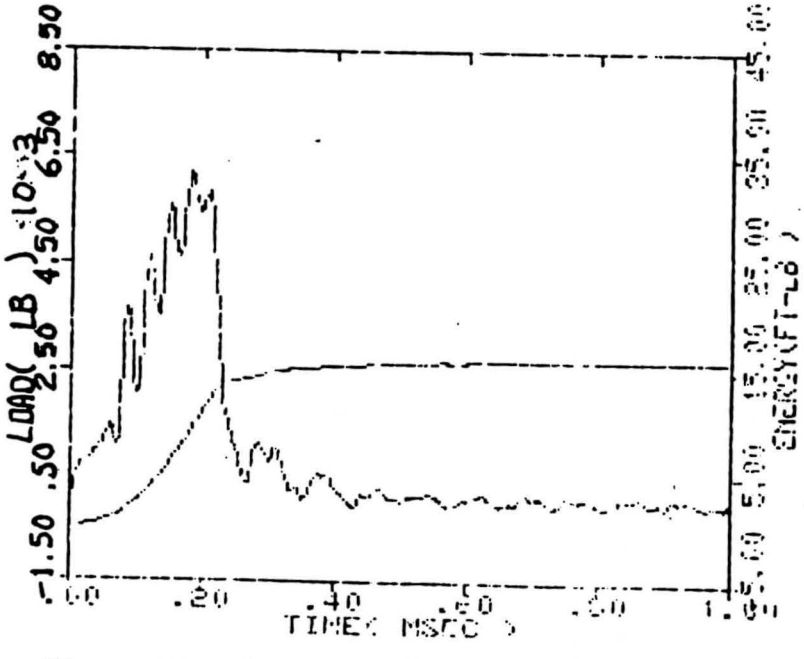

Figure 21: Specimen 18, heat 870494, standard, tape on tup, IE=11.0 ft-lb, TE=15.74 ft-lb, CVN=4.74 ft-lb

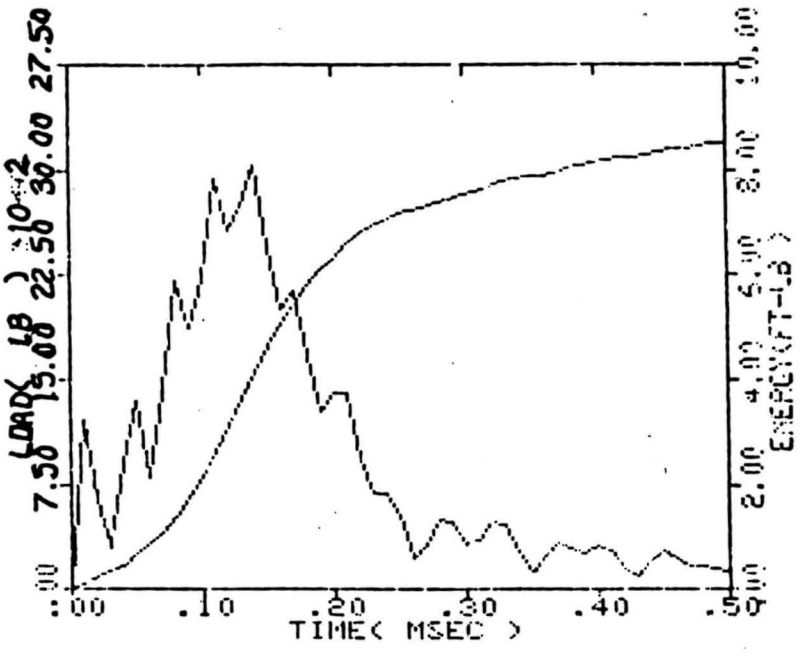

Figure 22: Specimen 19, heat 870494, precracked, no tape on tup, CVN=8.89 ft-lb

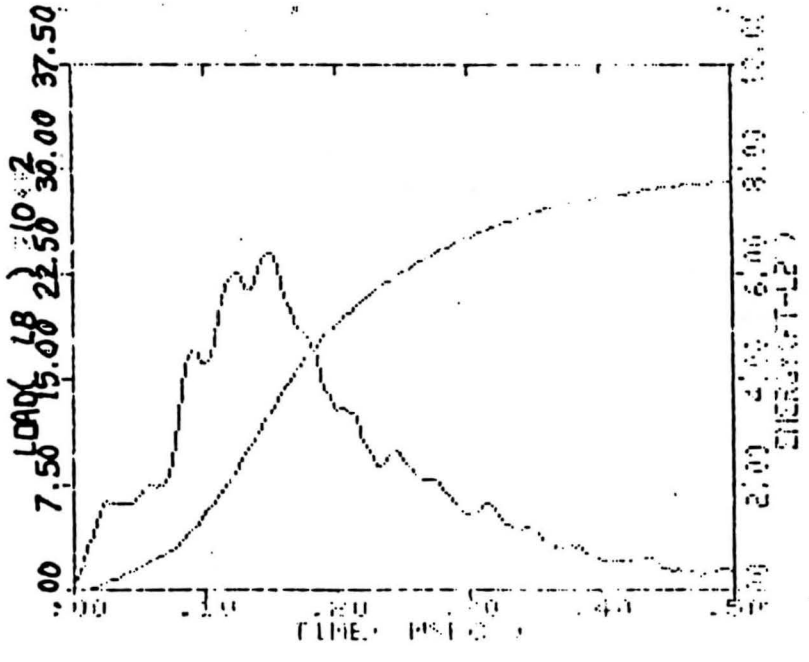

Figure 23: Specimen 20, heat 870494, precracked, tape on tup, CVN=8.20 ft-lb

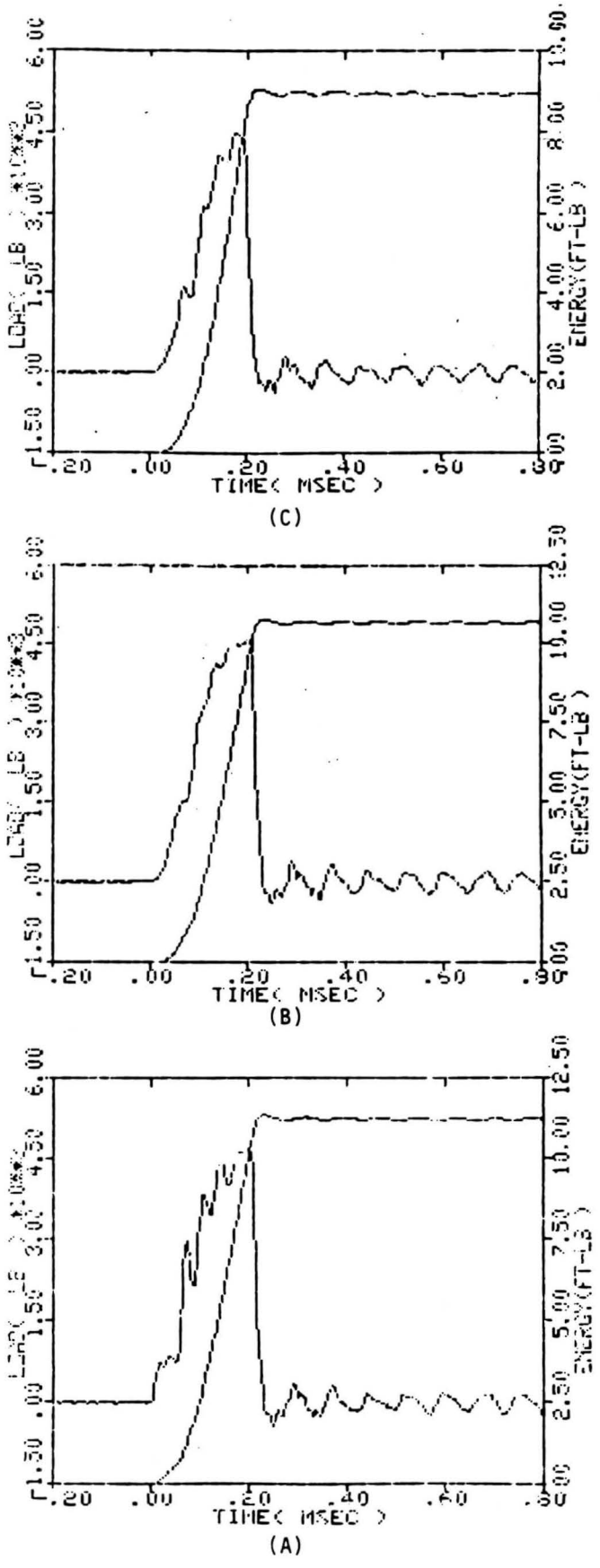

Figure 24: Curves showing affect of repeated use of the same piece of tape on the tup.
(A) First run with tape.
(B) Second run with tape.
(C) Third run with tape.

(Standard samples of 4340 steel were used for this demonstration.)

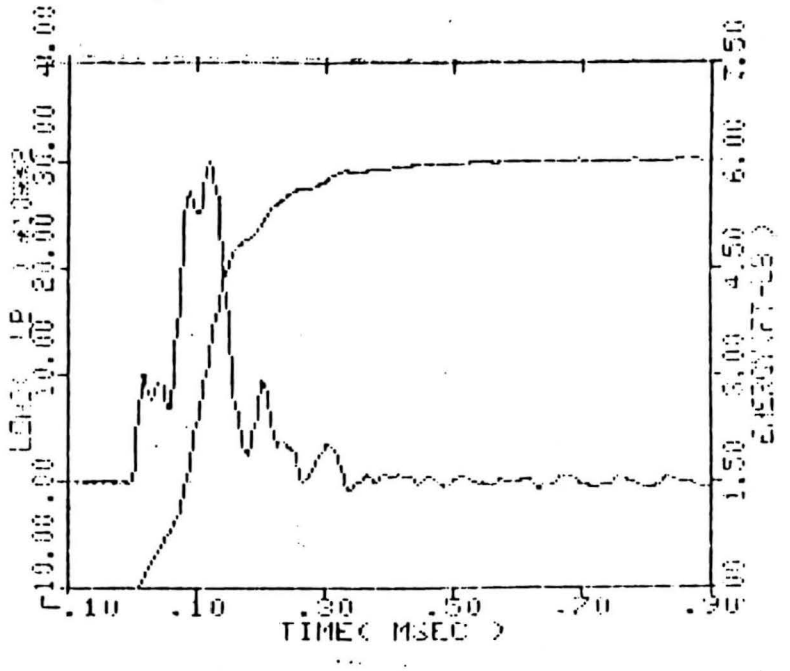

(A)

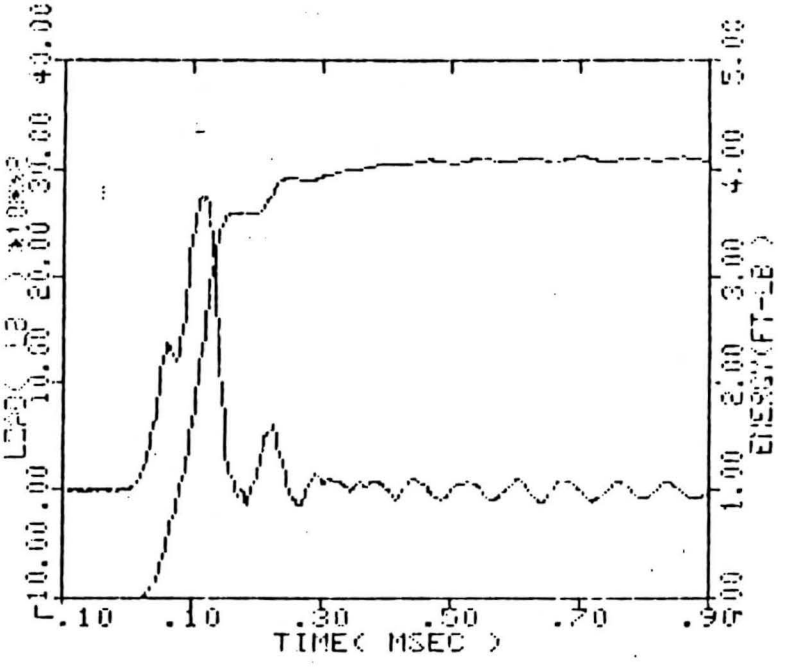

(B)

Figure 25: Curves showing effect of repeated use of the same piece of tape on the tup.
(A) First run with tape.
(B) Second run with tape.

(Standard samples of grey cast iron were used for this demonstration.)

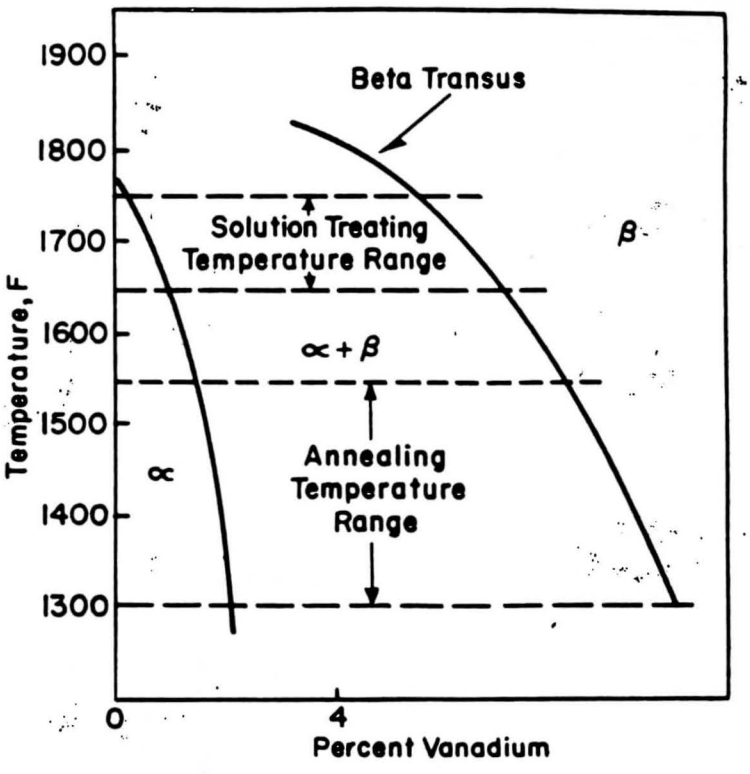

Figure 26: Partial Phase Diagram for Titanium 6Al-4V (Ref. 13)

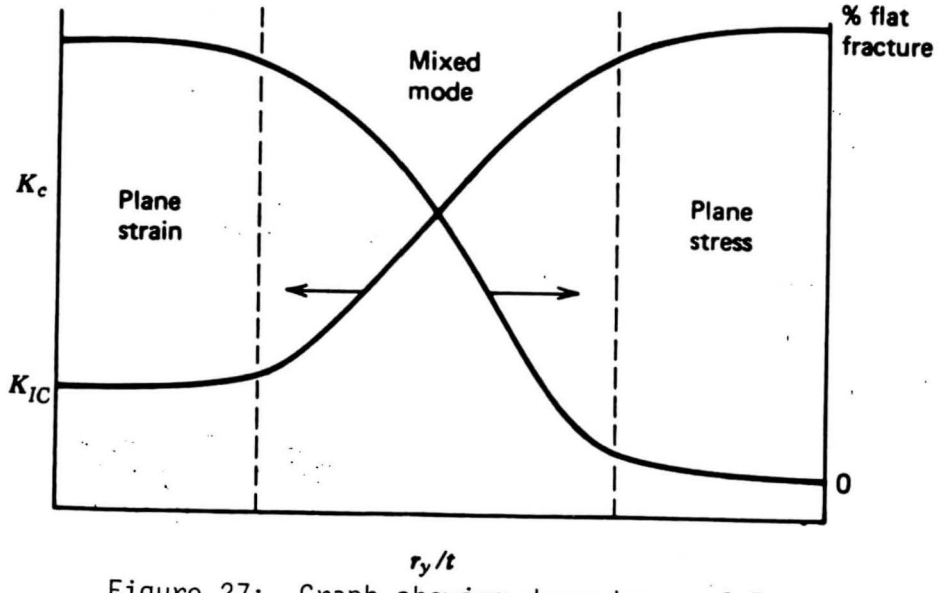

Figure 27: Graph showing dependance of Fracture Toughness on Percent Flat Fracture (Ref. 4)

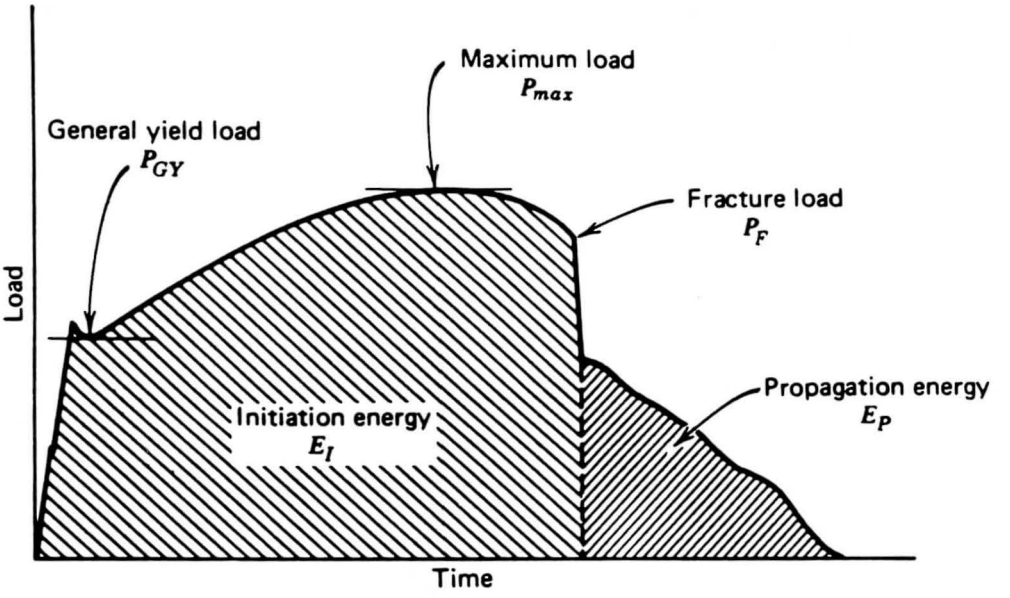

Figure 28: Load versus Time Curve for an Instrumented Charpy Impact Test showing the method of finding CVN_1. (Ref. 4)

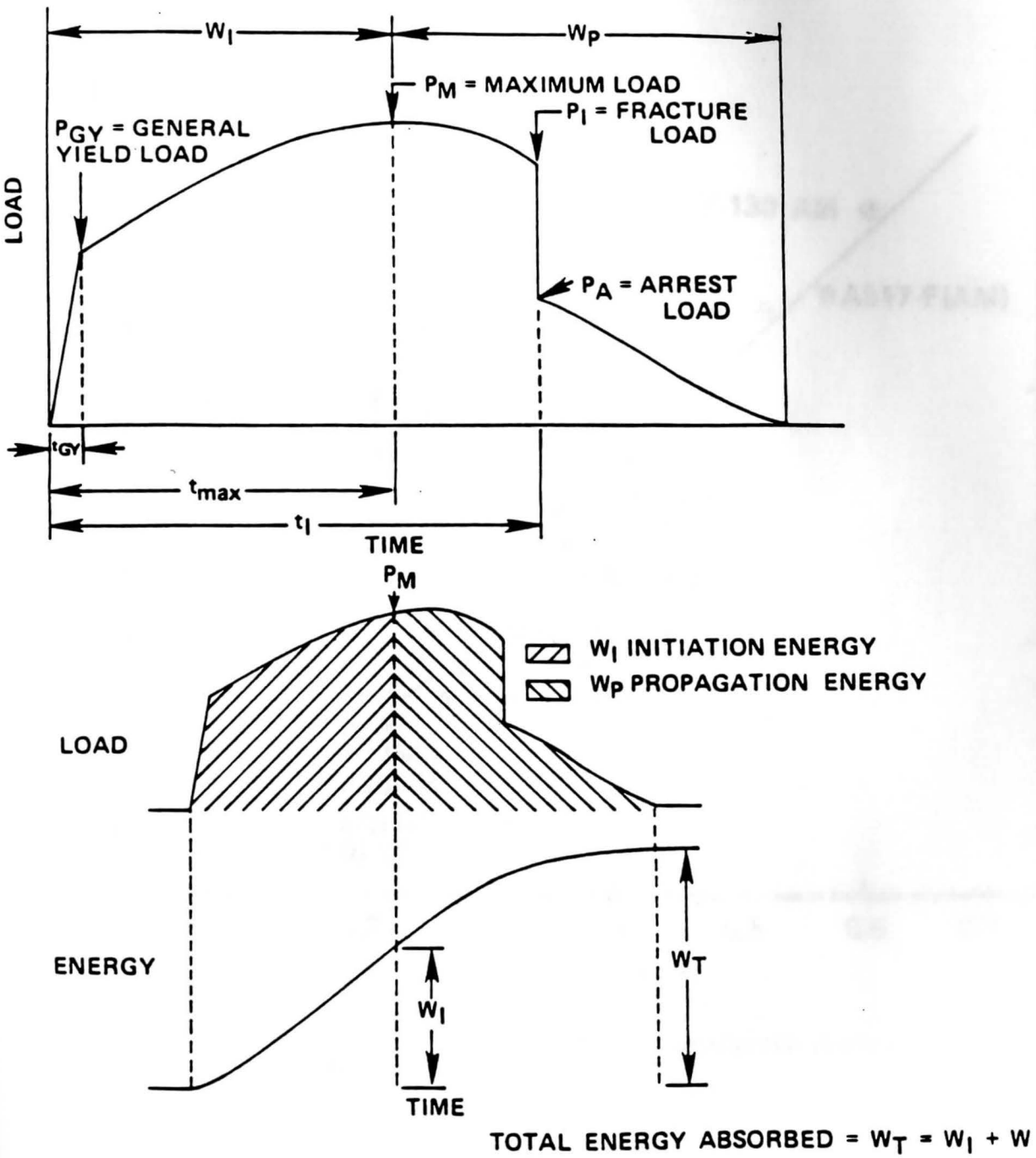

Figure 29: Load versus Time Curve for an Instrumented Charpy Impact Test showing the method of calculating CVN_2.

(Ref. 7)

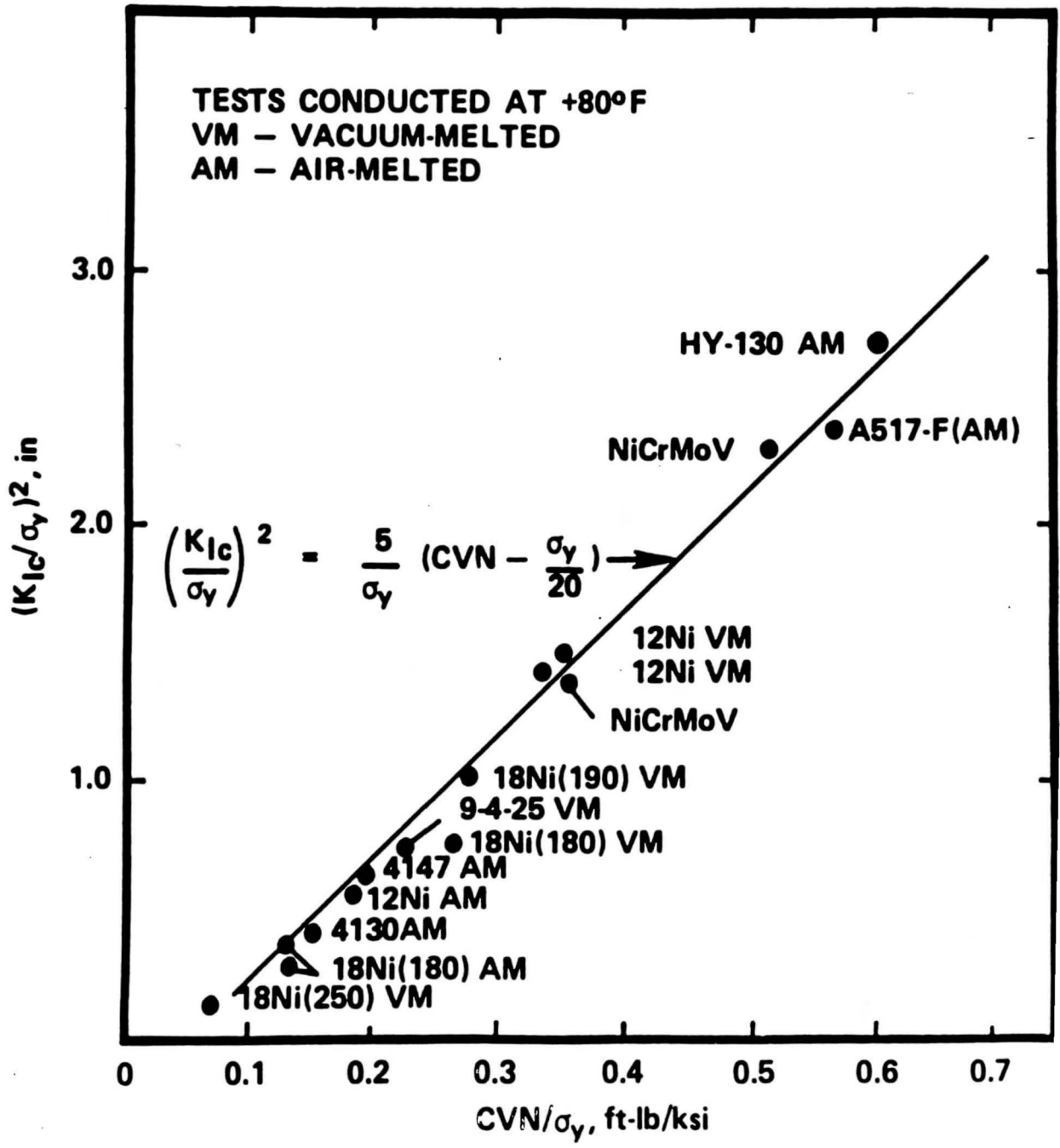

Figure 30: Curve showing the Rolfe-Novak-Barson correlation, (Ref. 5)

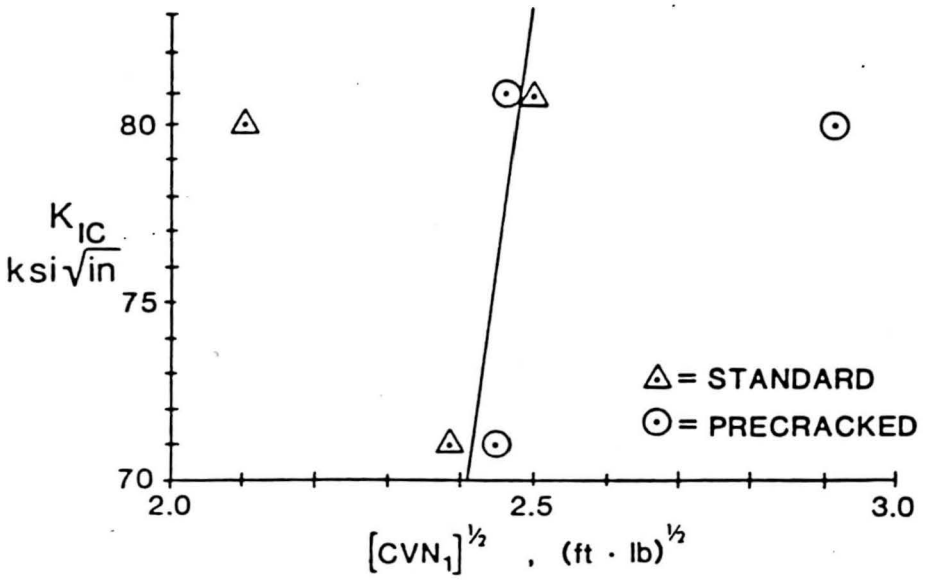

FIGURE 31: CORRELATION OF K_{IC} TO $[CVN_1]^{1/2}$

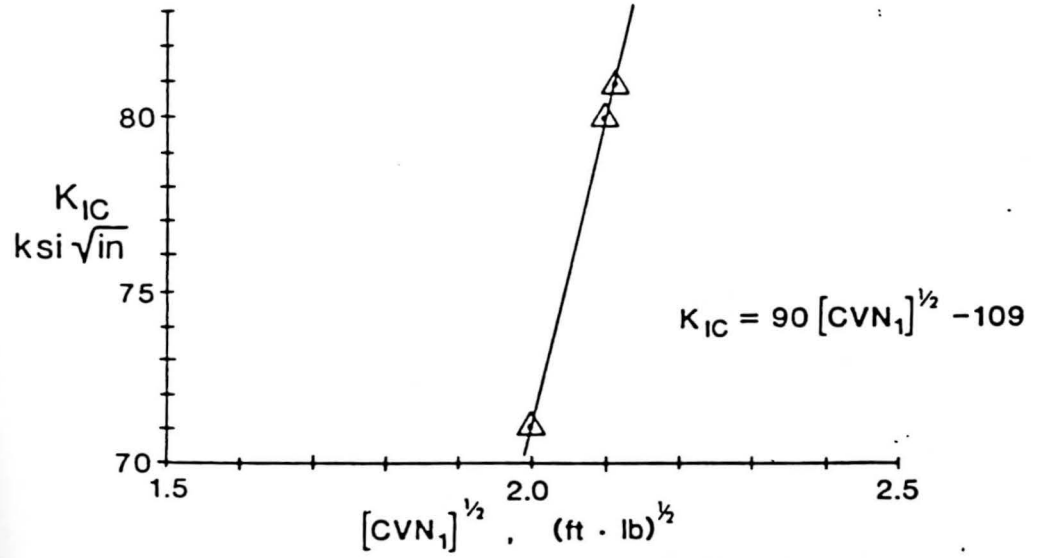

FIGURE 32: CORRECTED CORRELATION FOR STANDARD SPECIMENS

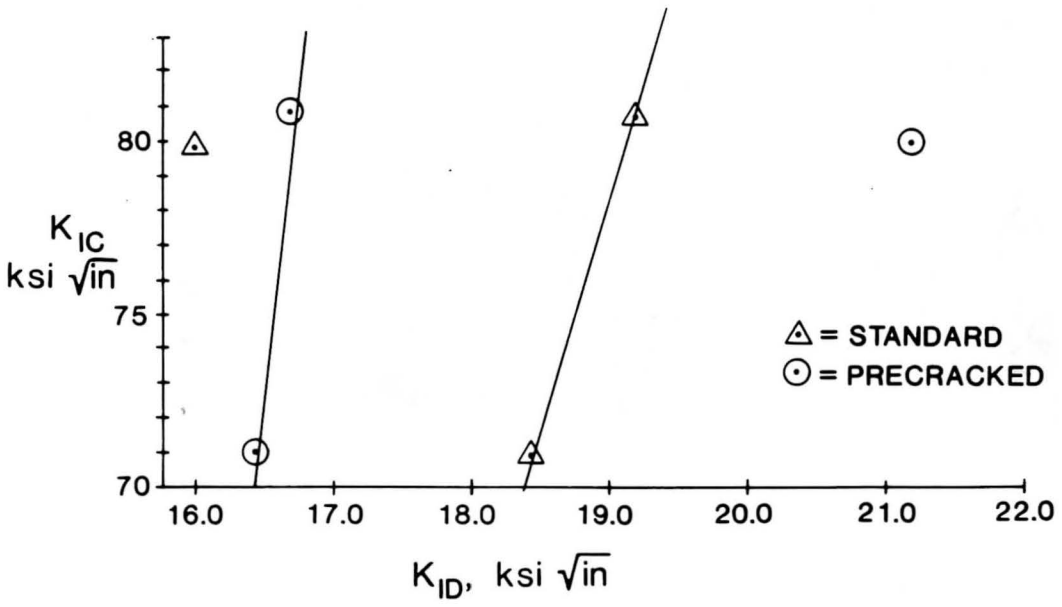

FIGURE 33: CORRELATION OF K_{IC} TO K_{ID}

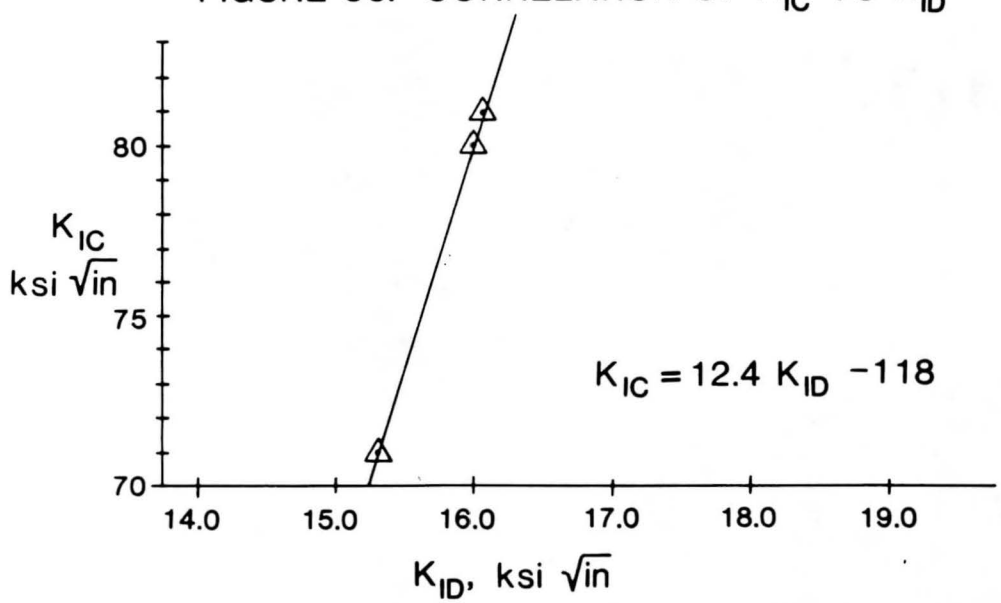

FIGURE 34: CORRECTED CORRELATION

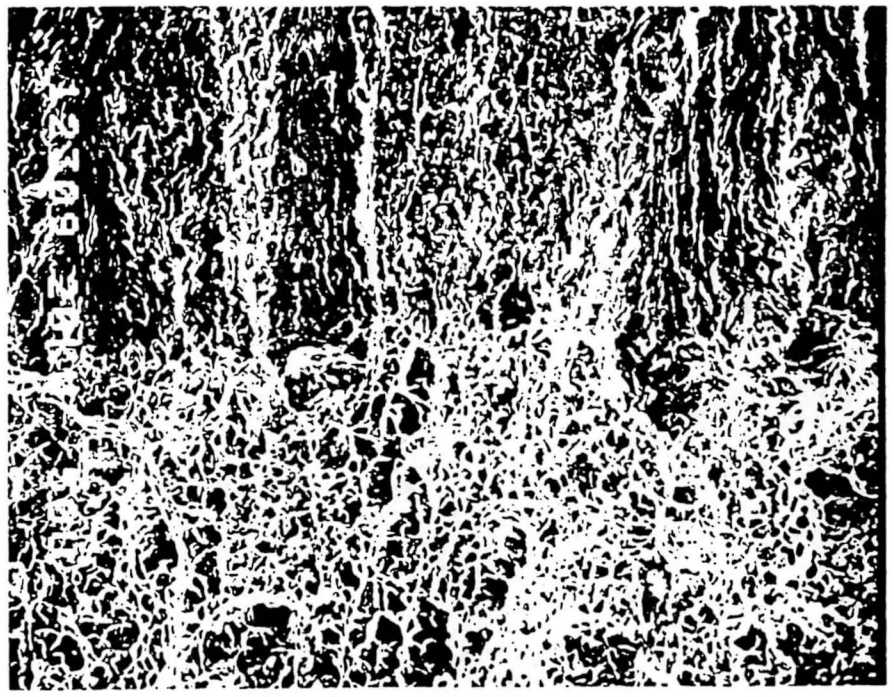

140 X

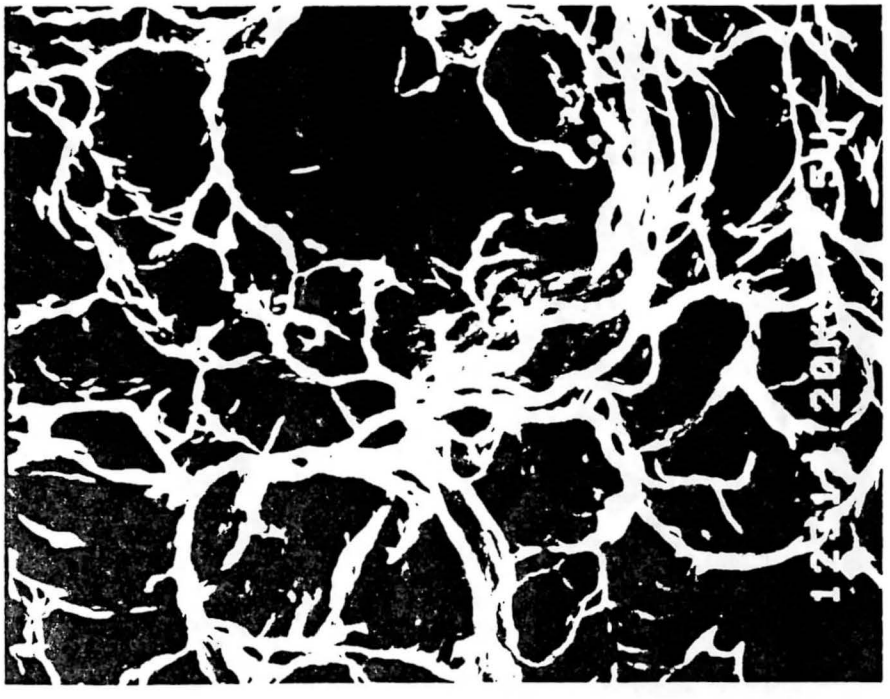

1400 X

Figure 35: SEM photomicrographs of fracture surface of heat 870488, top of 140X photo shows precracked zone while bottom shows fast fracture zone.

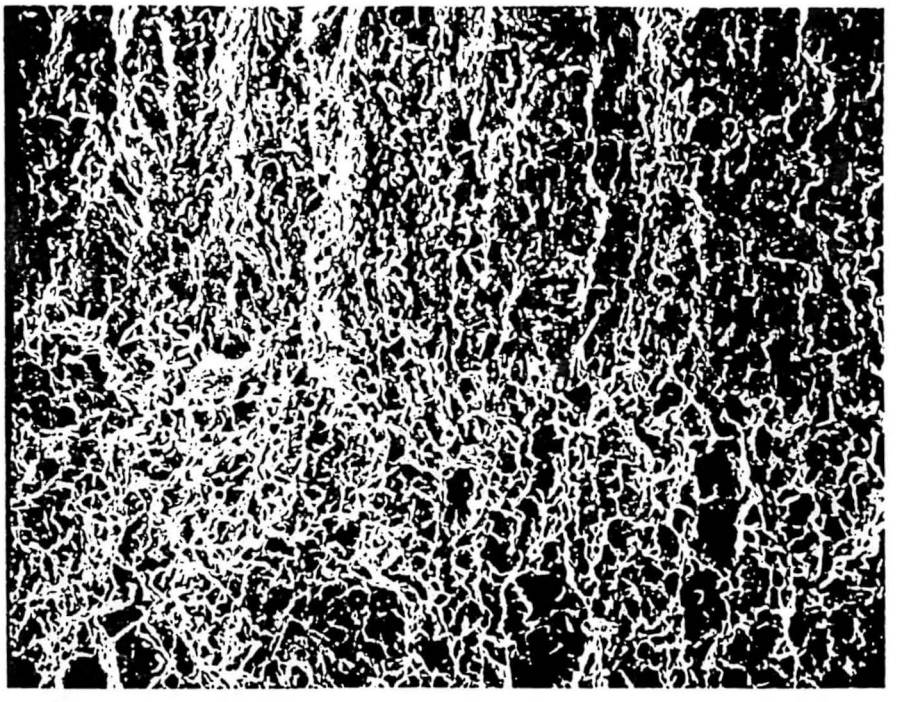

140 X

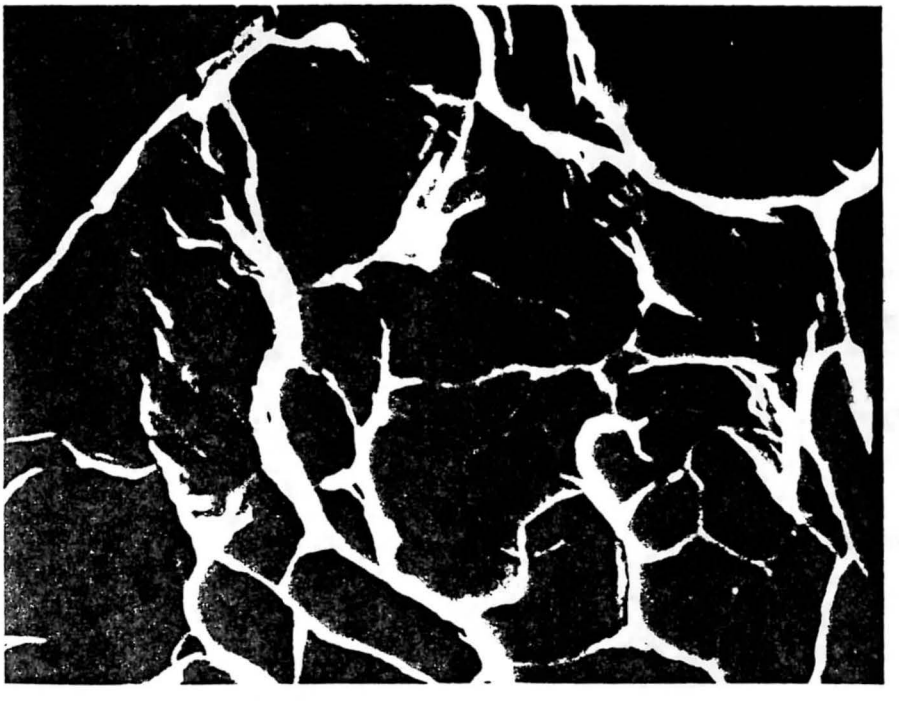

1400 X

Figure 36: SEM photomicrographs of fracture surface of heat 880423, top of 140 X photo shows precracked zone while bottom shows fast fracture zone.

40 X

140 X

Figure 37: SEM photomicrographs of fracture surface of heat 870494, top of 40 X photo shows precracked zone while bottom shows fast fracture zone.

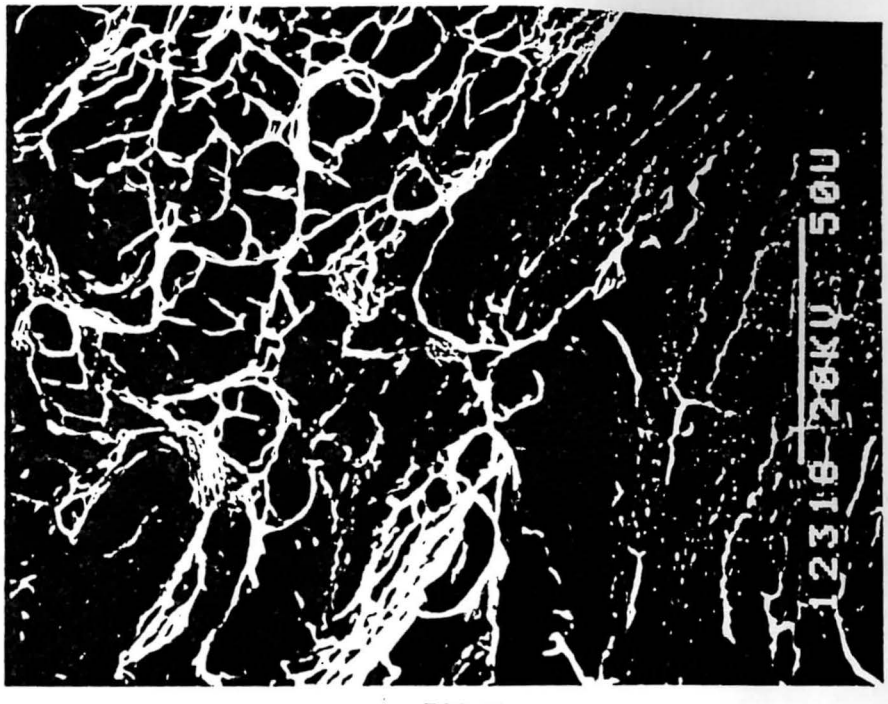

720 X

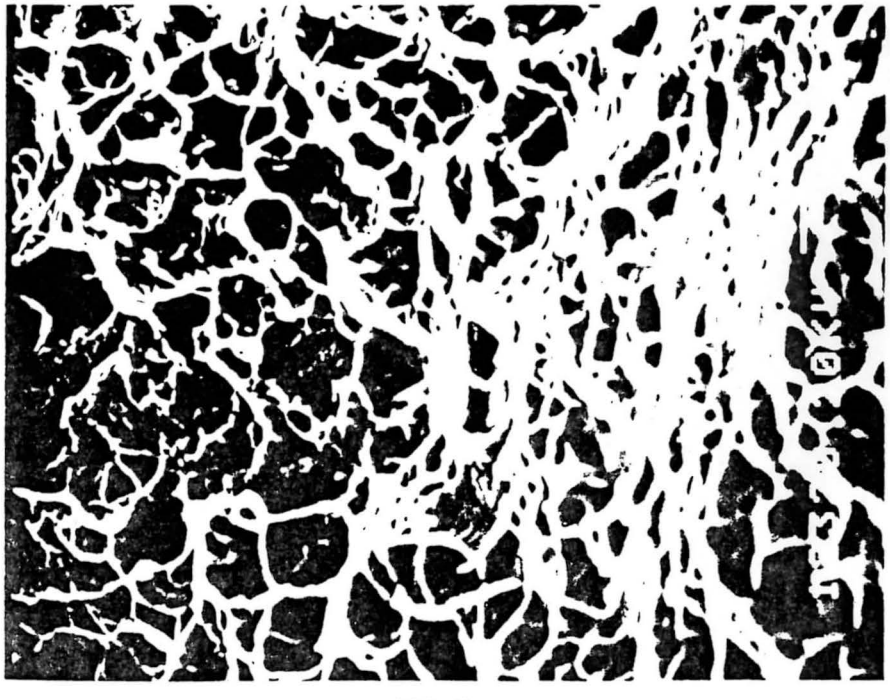

1400 X

Figure 37: continued.